Friction **8**(1): 4–28 (2020)
https://doi.org/10.1007/s40544-019-0356-5
ISSN 2223-7690
CN 10-1237/TH

REVIEW ARTICLE

Electrical bearing failures in electric vehicles

Feng HE, Guoxin XIE*, Jianbin LUO*

State Key Laboratory of Tribology, Department of Mechanical Engineering, Tsinghua University, Beijing 100084, China

Received: 08 September 2019 / Revised: 26 November 2019 / Accepted: 17 December 2019

Abstract: In modern electric equipment, especially electric vehicles, inverter control systems can lead to complex shaft voltages and bearing currents. Within an electric motor, many parts have electrical failure problems, and among which bearings are the most sensitive and vulnerable components. In recent years, electrical failures in bearing have been frequently reported in electric vehicles, and the electrical failure of bearings has become a key issue that restricts the lifetime of all-electric motor-based power systems in a broader sense. The purpose of this review is to provide a comprehensive overview of the bearing premature failure in the mechanical systems exposed in an electrical environment represented by electric vehicles. The electrical environments in which bearing works including the different components and the origins of the shaft voltages and bearing currents, as well as the typical modes of electrical bearing failure including various topographical damages and lubrication failures, have been discussed. The fundamental influence mechanisms of voltage/current on the friction/lubrication properties have been summarized and analyzed, and corresponding countermeasures have been proposed. Finally, a brief introduction to the key technical flaws in the current researches will be made and the future outlook of frontier directions will be discussed.

Keywords: electric vehicles; bearing; premature failure; electrical environment; shaft voltage

1 Introduction

The first concept electric car was exhibited in the 1830s, and commercial electric cars came out at the end of the 19th century [1]. However, compared with traditional internal combustion (IC) engine vehicles, electric cars showed disadvantages in limited mileage ranges, heavy batteries and difficulties to refuel [2–4]. Thus, electric vehicles were not successful once they came out. In terms of advantages, electric vehicles possess high reliability, high power density, high efficiency and the ability to start immediately [5]. At that time, a successful application of electric vehicles was the electric trolley bus powered by catenaries. Nowadays, the global energy crisis is becoming tougher, and the fossil energy reserves as the fuels of IC engines are limited and non-renewable [6, 7]. Moreover, the pollution of greenhouse gases (carbon dioxide) and other exhaust gases generated by IC engine vehicles is becoming increasingly more serious [8]. Along with the potential in fields of goods distribution and intelligent transportation systems, these problems make electric vehicles, which were once considered uncompetitive, an attractive role [9–11]. In addition, the technical field of electric vehicles has been greatly expanded in the past decades, and great progress has been made in tackling the key issues such as batteries, electric motor drives, automotive technology and system integration [12–16]. In the case of batteries, there have been unprecedented advancements in battery life, energy density, charge capacity, voltage output, energy efficiency, charging systems, etc. [17, 18]. As a result, automobile manufacturers have spared no effort in the field of electric vehicles to meet growing market demands. Meanwhile, the market share of electric vehicles is gradually increasing, and electric

* Corresponding authors: Guoxin XIE, E-mail: xgx2014@tsinghua.edu.cn; Jianbin LUO, E-mail: luojb@tsinghua.edu.cn

vehicles have begun to replace IC engine vehicles in China, European and USA [19–21]. So far, electric vehicles can be divided into five types: traditional battery electric vehicle (BEV), hybrid electric vehicle (HEV) or plug-in hybrid electric vehicle (PHEV) (equipped with both IC engine and electric motor), fuel cells battery electric vehicle (FCEV), solar battery electric vehicle (SEV) and electric vehicle powered by supply lines [1, 22, 23]. Although there have been great innovations in propulsion systems (different power sources and converters), these electric vehicles have similar motor drive systems: A DC/DC converter for reducing the voltage, an inverter for driving the motor, and an electric motor (Fig. 1). Consequently, the reliability of electric vehicles is greatly limited by the stability of the motor system. Motors used in electric vehicles include DC motor, induction motor, permanent magnet motor, PM brushless DC motor and switched reluctance motor, etc. [26–28]. Among them, the three-phase induction motor is by far the most widely used prime mover [29, 30]. Regardless of the motor type, there will be shaft voltages and currents generated during rotation, which was first discovered in the 1920s [31, 32]. Moreover, the common application of the inverter, which is used to convert the DC voltage of the battery into an AC voltage in the electric vehicles, exacerbates this problem [33–35].

The induced shaft voltages and currents can cause premature failure problems in a series of components such as bearings, seals, pads, and gears, and they can also give rise to electromagnetic interference (EMI) and radio frequency interference problems making the motor unstable [36–39]. Even with the performance improvement of the adjustable speed inverters, the lifetime of the electric motor is further reduced. In comparison, the premature failure problem of the bearings is the most serious, and it was reported that over 40% of motor failures were attributed to bearing failure [40, 41]. In recent years, many lubrication failure problems owing to shaft voltages and bearing currents have been reported, and these problems will lead to instability, vibration and noise of a bearing, and consequently, more serious mechanical failures [42–46]. It is reasonable to expect that the electrical

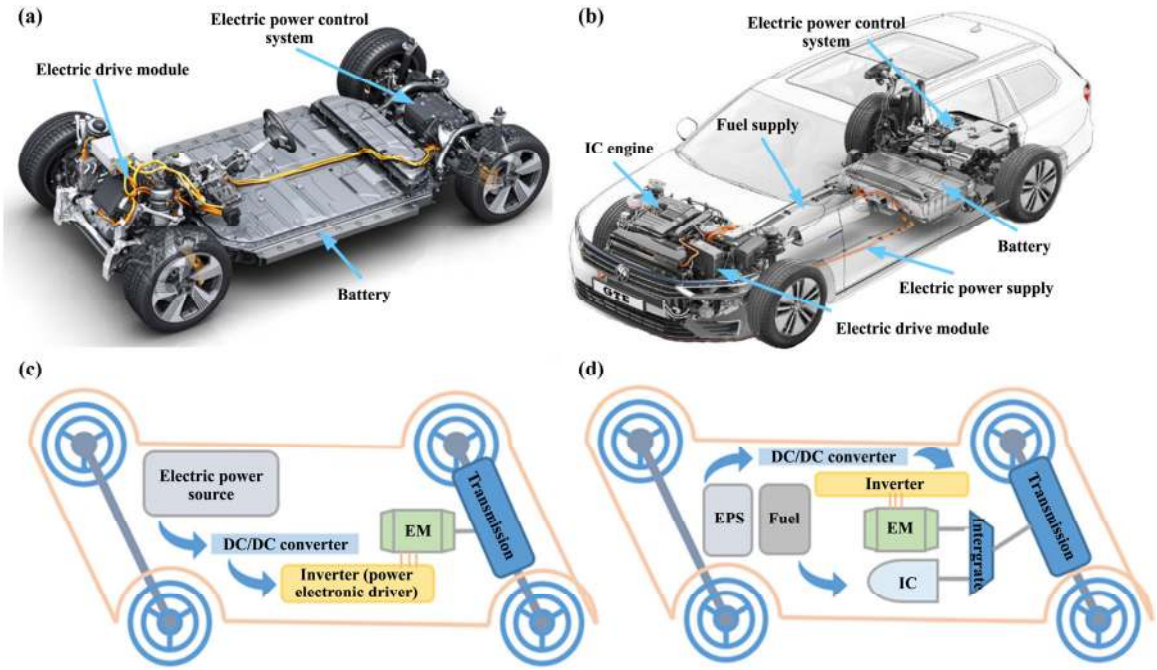

Fig. 1 The key components of electric vehicles' drivetrain. (a) A battery-electric vehicle. Reproduced with permission from Ref. [24], ©Springer Nature 2019. (b) A hybrid electric vehicle. Reproduced with permission from Ref. [25], © Springer Nature 2015. (c) Typical electric vehicles without internal combustion (IC) engine, which can be divided into FCEV, SEV, and BEV according to the internal components of the electric power source. The order of energy transfer: electric power source (EPS), DC/DC converter (adjust and stabilize the DC voltage output), inverter, electric motor (EM) and transmission. (d) HEV with both electric motor and IC engine. On the basis of (c), the fuel-IC engine-transmission path is added.

failures in bearings will gradually emerge with the popularity of electric vehicles in the near future. Under these circumstances, in order to ensure the long-term stability of the bearings in electric vehicles, it is of great industrial and scientific significance to deepen and update the influences of an electric environment on the bearing-lubrication system.

This paper provides a detailed review of the key research progresses on the electrical bearing failures. Specifically, the review consists of four stages: Firstly, the origin of electric failures: the generation of shaft voltages in electric vehicles will be summarized in **Section 1**; the electrical model of a motor and various bearing current responses under different shaft voltages will be reviewed in **Section 2**. Secondly, different appearances of electrical bearing failures will be discussed in **Section 3**; Thirdly, the fundamental researches on the lubrication performance in an electrical environment will be provided in **Section 4**. Fourthly, the solutions to suppressing or avoiding electrical bearing failures will be introduced in **Section 5**. Finally, brief comments on the current research progress will be given and a future prospect of failure researches in an electrical environment will be proposed.

2 The origin of electrical bearing failures: shaft voltages and bearing currents

2.1 The electric source-shaft voltages

In electric motors, electrical failures such as electric discharge machining (EDM) caused by electromagnetic and electrostatic effects are unavoidable. To further understand these electric phenomena, a basic understanding of shaft voltages (the source of electrical failures) is needed. Here, the shaft voltages are divided into three parts according to their generation: magnetic flux asymmetry, electrostatic effects, and inverter-induced voltage effects.

2.1.1 Magnetic flux asymmetry

Magnetic asymmetry arises due to the deviations in the magnetic pole distribution or shaft position during design, manufacture or installation (Fig. 2(a)). Specifically, the reasons include asymmetrical windings, rotor eccentricities, casting defects, uneven permeability, unbalanced voltage signal generated by the inverter, etc. [47–50]. As a result, compared with the symmetrical operating state (Fig. 2(b)), the shaft will form a voltage during the rotational process of cutting the magnetic induction line (Fig. 2(c)). These voltage/current waves are usually sinusoidal and of low frequency [51].

2.1.2 Electrostatic effects

The triboelectrification effect is due to the contact/friction behavior of dissimilar materials, especially on the surfaces of dielectric materials, where charges tend to accumulate and persist for a while [52]. In electric vehicles, in order to reduce weight, composite materials and polymer materials of dielectric nature are widely used, for example, body structural parts made of carbon fiber reinforced plastics (CFRP), the cooling systems made of high thermal conductive insulating polymers and sealing rings made of rubber. In these components, triboelectrification can induce significant charge separation between the surfaces and accumulate considerable electrostatic charges [53]. When the electrostatic field reaches the breakdown strength of air or the lubricant, the accumulated charges are released to form discharge currents (Fig. 2(d)), which is known as the forming process of EDM current.

2.1.3 Inverter-induced voltage

In modern electric vehicles, the pulse-width-modulation (PWM) inverters with fast switching devices such as metal-oxide-semiconductor field-effect transistor (MOSFET) and insulated gate bipolar transistor (IGBT) are widely used in electric motors to achieve variable-speed-control [54]. The high-frequency switching rate of the inverters will induce high-frequency common mode voltage (CMV), which is defined as the voltage between the motor neutral and the stator core (ground). As shown in Fig. 2(e), a three-phase induction motor is driven by a typical adjustable speed drive which contains a three-phase inverter [55], and the CMV (voltage at N in Fig. 2(e)) is equal to one-third of the vector sum of the voltages in three individual phases. If the voltage output from the inverter is a symmetrical sinusoidal signal, the CMV will remain at zero (Fig. 2(f)). However, the inverter often uses a

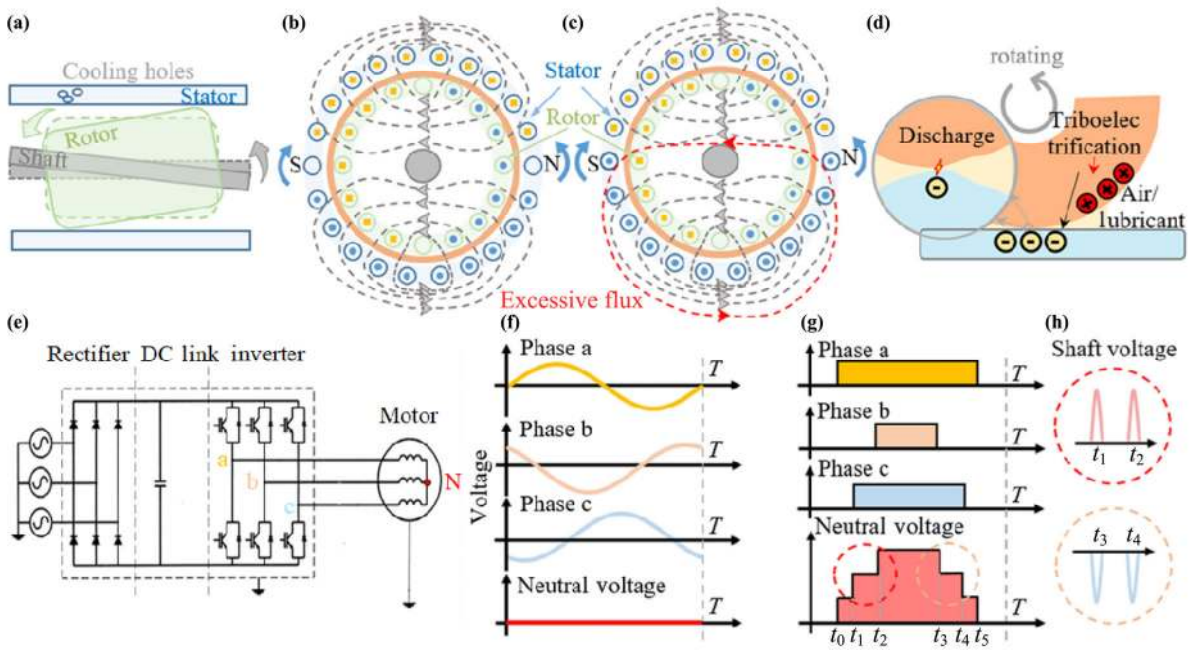

Fig. 2 Generation mechanisms of shaft voltages. (a–c) Magnetic flux asymmetry: (a) asymmetries of stator, rotor, and shaft during relative motion; (b) normally working induction motor; (c) working condition with unbalanced flux; (d) electrostatic effects: discharge induced by triboelectrification. (e–f) Inverter-induced voltages: (e) Circuit configuration of an induction motor driven by a typical adjustable speed drive which contains a three-phase inverter. Reproduced with permission from Ref. [55], © Elsevier 2001. (f) When the three-phase signals are of symmetrical sinusoidal waveforms, the neutral voltage is maintained at zero. (g) Stepped neutral voltage (CMV) when the three-phase signals are of pulse-width modulation waveforms. (h) Shaft voltages are induced at the steps of CMV.

pulse waveform to simulate a sinusoidal waveform, the series of pulse waveforms of a three-phase inverter are asymmetrical, and thus forming a stepwise CMV (Fig. 2(g)). Similarly, although there is no neutral point in delta-winding-connected electric motor, the unbalanced output of the inverter still causes "common mode" effects. Further, shaft voltages are induced by capacitive and magnetic coupling at the step positions of the CMV waveform (Fig. 2(h)). In terms of control, the higher the switching frequency, the more the CMV conforms to the sinusoidal waveform, as well as lifting efficiency [56]. In terms of shaft voltage, the high switching frequency means the high $\mathrm{d}v/\mathrm{d}t$ in CMV waveform, introducing the high-frequency harmonic distortion in the motor system, inducing the high-frequency shaft voltage with a large amplitude [57]. Such a high-frequency shaft voltage could be harmful because it can pass through many interfaces even if they are insulated.

2.2 The generation of bearing currents

In a typical induction motor, a complex capacitor system exists due to the presence of air gaps, insulation coating, and lubricants, including the aggregate stator windings to the stator frame (C_{ws}), the aggregate stator winding to the rotor (C_{wr}), the rotor the frame (C_{rf}), the bearings (C_{bf}, C_{be}), the stator to the rotor (C_{sr}), the rotor to ground (C_{rg}), etc. [58, 59]. Moreover, when a capacitor breaks down, it turns into resistive. Figure 3(a) shows the simplified physical schematic and corresponding circuit models of an induction electric motor, and the possible current paths caused by different voltage sources are also very complicated. As for the current sources, bearing currents can be divided into "circulating" and "non-circulating" [60, 61].

2.2.1 *"Non-circulating" currents*

The "non-circulating" types of currents include the $\mathrm{d}v/\mathrm{d}t$ related currents and "electrical discharge machining (EDM)" current pulse (Fig. 3(b)). It is termed "non-circulating" because these currents pass through the bearings unidirectionally from the rotor to the stator [60].

The $\mathrm{d}v/\mathrm{d}t$ related currents can be conductive and

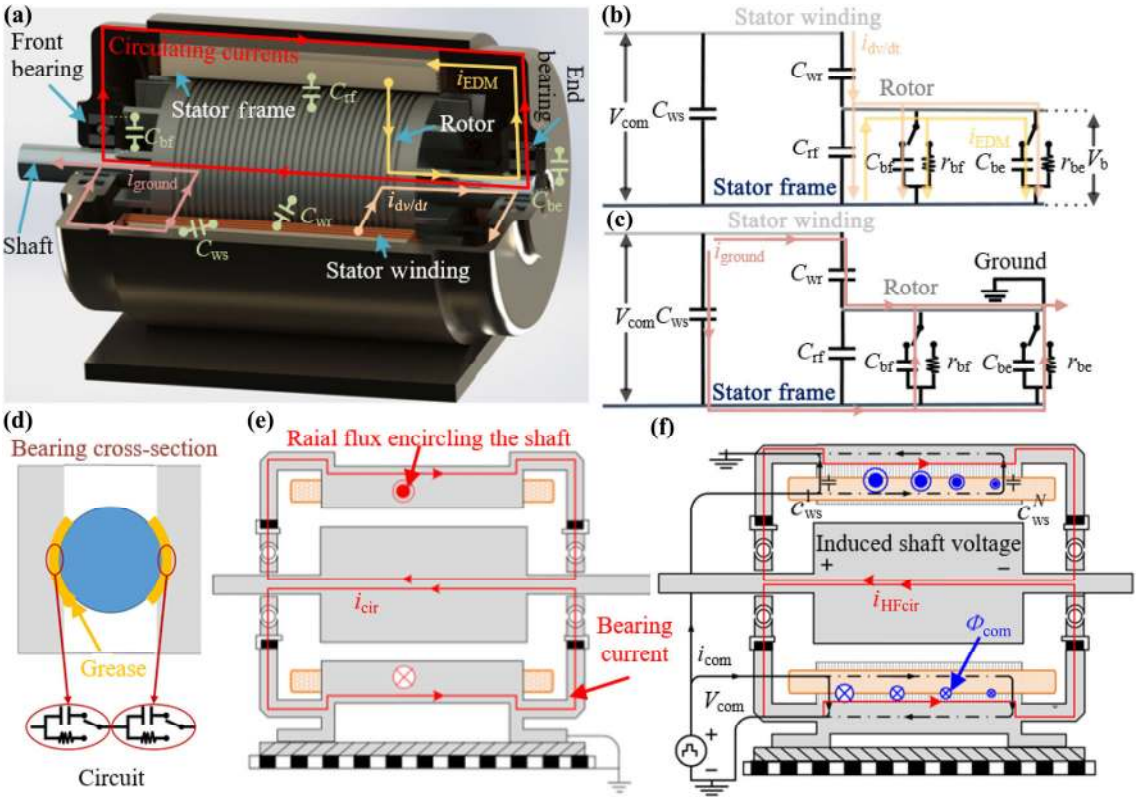

Fig. 3 The occurrence of bearing currents and their possible paths. (a) Simplified physical schematic and circuit models of an induction electric motor. (b) Circuits of dv/dt related currents ($i_{dv/dt}$) and EDM currents (i_{EDM}). (c) Circuits of grounding currents (i_{ground}). (d) Equivalent circuit model of a bearing. (e) Classical low frequency circulating current (i_{cir}). Reproduced with permission from Ref. [72], © Institution of Engineering and Technology (IET) 2017. (f) Path of common mode current (i_{com}) induced by CMV (V_{com}), resulting in magnetic field distribution (Φ_{com}) and high-frequency circulating current (i_{HFcir}). Reproduced with permission from Ref. [72], © IET 2017.

capacitive [62]. The conductive currents mainly occur when the motor is running at a low speed. Since an effective insulating film cannot be maintained at low rotational speeds, the internal contact of the bearing is metallic. Thus, the current flowing from the stator winding appears to be conductive in the bearing. At normal rotational speeds, the insulating lubricate oil/grease film electrically works as a capacitor [63]. When switching occurs in the IGBT, as long as the switched voltage does not cause a breakdown, the capacitor of the bearing is charged or discharged. Specifically, the high-frequency (corresponding to the switching frequency) current passes through the stator winding to the rotor, then to the bearing, and finally to the frame (Figs. 3(a) and 3(b)). However, the magnitude of dv/dt related currents are small, and the capacitive ones are only 5–10 mA, while the conductive ones do not exceed 200 mA [64]. Therefore, dv/dt current components are often harmless and only account for a small percentage of all bearing currents.

EDM bearing currents occur when the bearing voltage exceeds the threshold voltage of the insulating lubricating film, and the energy of the capacitor is released by destructive currents and arcing [65]. As mentioned above, the bearing works as a capacitive voltage at normal rotational speeds (Fig. 3(d)). Bearing voltage (V_b) can be estimated from CMV (V_{com}) and bearing voltage ratio (BVR) [66]:

$$V_b = \mathrm{BVR} \cdot V_{com} = \frac{C_{wr}}{C_{wr} + C_{rf} + C_{bf} + C_{be}} \cdot V_{com}$$

Generally, BVR ranges from 3% to 10% [58]. In consideration that the voltages of AC supplies in electric vehicles are at least 300 V, the peak of bearing voltage can reach ~30 V. The lubricant film thickness in bearings commonly ranges from 0.1 to 1.4 microns, which can withstand voltages ranging from 1.5 to

21 V (dielectric strength: 15 V/μm) [67, 68]. Thus, the electrical breakdowns are likely to occur, giving rise to the generation of the EDM currents. With the nature of short-circuit current, the amplitude of the EDM currents in a 1.5 kW induction motor can range from 0.2 to 1.4 A [69]. The path of the EDM currents is "shaft-inner race of the bearing-rollers-outer ring-frame" [70]. Different from dv/dt currents, which happen at switching moments, the occurrence of EDM currents is not directly related to the rise time of the CMV wave. In actual working conditions, the lubricant film thickness is affected by speed, load, and lubricant viscosity. Moreover, the surface roughness at the bearing interfaces, the uniformity of lubricant distribution, the history of discharge, and the fluctuations of mechanical operation also contribute to the discharge. For these reasons, although high CMV can result in an increased probability of the EDM currents, the occurrence of the EDM currents is more likely to be random [71].

In special cases, when the rotor-to-ground resistance is smaller than the stator-to-ground resistance, part of the bearing current will flow to the ground through the shaft, following "stator – bearing – rotor shaft – ground" (Figs. 3(a) and 3(c)).

2.2.2 *"Circulating" current*

Compared to the "non-circulating" type, the generation of the "circulating" type current is far more complicated, involving magnetic induction, inductive coupling and capacitive coupling [60]. The earliest "circulating" current was found in the sine-wave-operated AC motor, which is also known as the classical inductive bearing current [31]. This kind of "circulating" current mostly occurs owing to magnetic flux asymmetry, and the frequency corresponds to the shaft speed. As shown in Fig. 3(e), when the induced shaft voltage is strong enough to break through the oil film/grease in a bearing, the bearing current would circulate in a conductive loop, i.e., "stator – drive end bearing – rotor shaft – non drive end bearing – stator" [72]. In recent years, the classical induced bearing current is no longer considered to be a main current component due to the improvement of manufacturing and assembly processes. As reported by Maki-Ontto and Muetze, another kind of "circulating" current was derived from the CMV of the inverters: The parasitic capacitances between the stator winding turns and the frame are excited by the steep edges of high-switching-frequency CMV, generating a high-frequency common mode current which flows through the core of stator [73, 74]. Therefore, the current flowing into the stator winding is higher than the current flowing out. By taking a Gaussian surface inside the stator core perpendicular to the axis which encloses all the windings, the enclosed current is not zero due to the loss. In other words, there is an axial net current in the stator winding. According to Gauss' Law, there must be a net flux surrounding the shaft. As shown in Fig. 3(f), the high-frequency net current generates a high-frequency tangential magnetic flux (Φ_{com}) along and around the motor shaft, inducing the generation of the shaft voltage. Meanwhile, the induced bearing currents share similar formation processes and circulation to the first kind of the current. However, unlike the first kind, the frequency of this current can be as high as several megahertz, and the peak amplitude of this type of current is generally 0.5–20 A [60, 74].

In addition, there are some differential-mode bearing currents reported in the literature. Nippes et al. studied the water vapor droplets induced frictional electrification and discharge [37]. The grounding properties of different components also lead to different current paths and amplitudes [75]. Thus, many researches have been carried out to model the bearing currents under different electric parameters [76–78]. In comparison, the EDM currents and the high-frequency "circulating" current are the largest, accounting for the highest bearing current ratios, while other types of bearing currents receive less attention.

3 Electrical failures of bearings

Under a complicated electric environment, failure would occur on all contact/sliding surfaces of components, in which bearings are the most vulnerable. Thus, the bearing could be a typical example for illustrating such failures. The traditional bearing failure modes can be grouped into the following categories: fatigue spalling, fretting, smearing, skidding, abrasive

wear, corrosion, cracks, true or false brinelling, etc. [79]. In addition to these failure modes, the presence of shaft voltages and bearing currents can cause new failure modes [80]. Generally, the electric-related failure modes can be mainly divided into two parts: morphological damages and the influence on the lubrication process, corresponding to static results and dynamic processes, respectively (Fig. 4).

3.1 Morphological damage

Morphological damage due to shaft voltages and bearing currents can be classified into five types: frosting, fluting, pitting, spark tracks, pitting and welding.

3.1.1 Frosting

Frosting originates from weak but dense discharges. Owing to the satin-like appearance, a frosted surface is difficult to distinguish with the naked eye (Fig. 5) [32]. However, microscopically, this sand-blasted surface is composed of small "craters", and each "crater" indicates a melting effect when an EDM current occurs. Meanwhile, the surface area to volume ratio of a frosted bearing race increases, enhancing the subsequent chemical corrosion.

3.1.2 Pitting

Similar to frosting, pitting is also composed of "craters". However, the discharge is more intense. As a result of the single discharge pulse which has a larger current amplitude and lasts longer, the "craters" in pitting have a larger size (Fig. 6). In terms of distribution, the corroded pits corrosion appears as a random pattern, and they are sparser than frosting [88]. Komatsuzaki et al. reported that the key factor of the electrical pitting process was bearing current rather than shaft

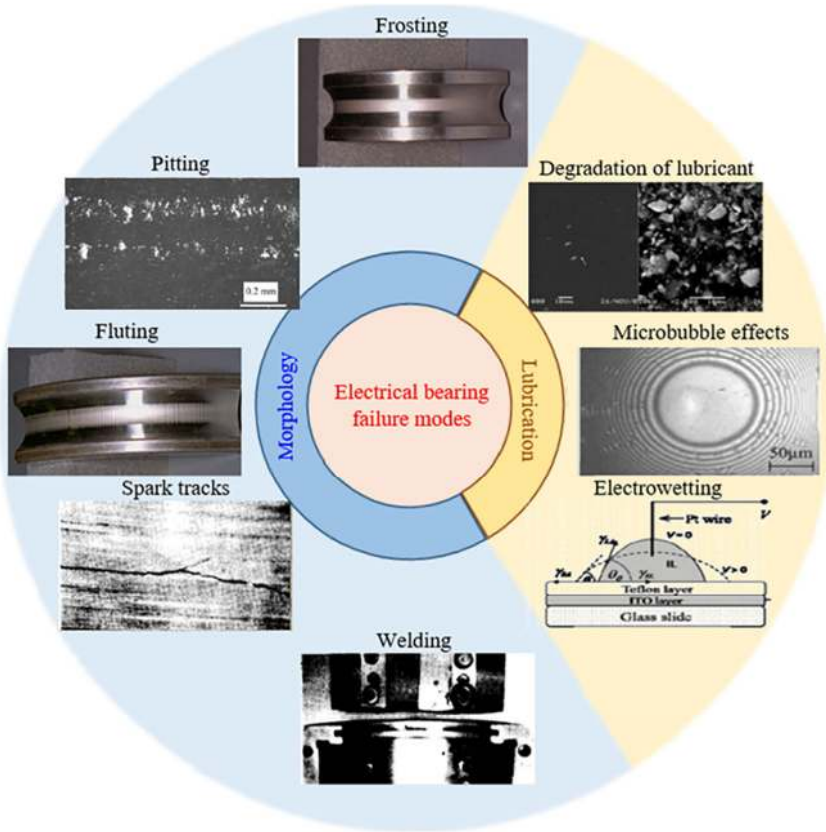

Fig. 4 The appearance and classification of the typical electrical bearing failures. Frosting and fluting, reproduced with permission from Ref. [43], © IEEE 2002. Pitting, reproduced with permission from Ref. [81], © Taylor & Francis 2011. Degradation of lubricant, reproduced with permission from Ref. [82], © Springer Nature 2010. Microbubble effects, reproduced with permission from Ref. [83], © Springer Nature 2008. Electrowetting, reproduced with permission from Ref. [84], © American Chemical Society (ACS) 2010. Spark tracks and welding, reproduced with permission from Ref. [85], © IEEE 1991.

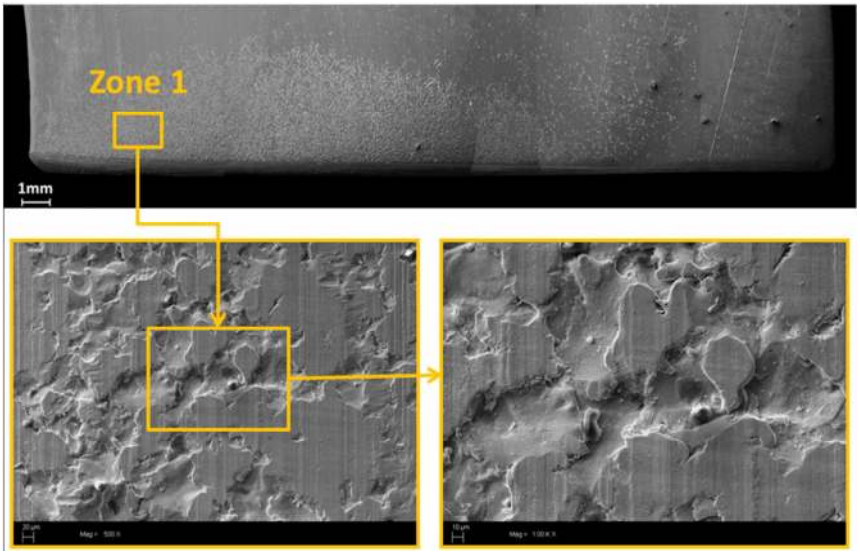

Fig. 5 A representative frosted bearing raceway. Reproduced with permission from Ref. [86], © Elsevier 2016.

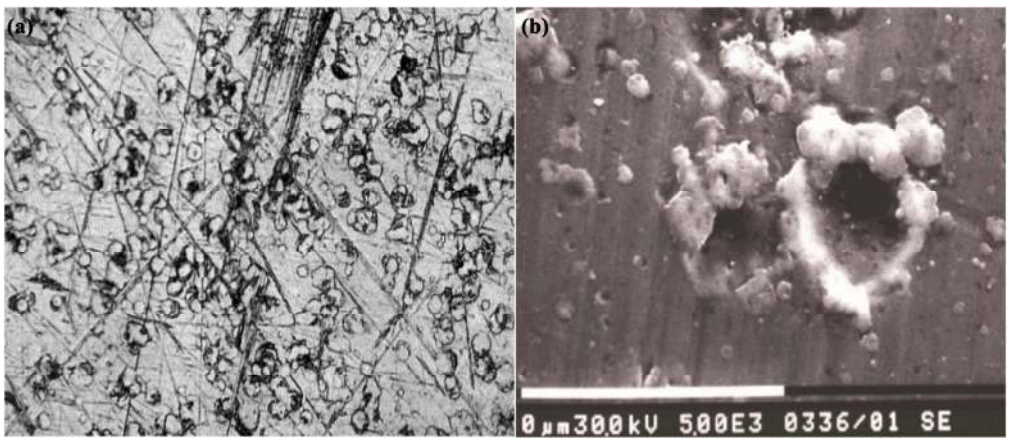

Fig. 6 Pitting. (a) A magnified view of micropitting. (b) A highly magnified view of micropits. Reproduced with permission from Ref. [87], © IEEE 2017.

voltage, and a 90 mA current was sufficient to cause pitting [89]. Chiou et al. investigated the formation mechanism of electric pitting: at a constant film thickness, the interface power increases with the increasing bearing currents, and the relationship between the pitting area A_p (in unit of 10^3 μm^2) and the interface power P (in W) is cubic function [90]:

$$A_p = 0.0059P^3 - 0.068P^2 + 0.46P.$$

In consideration of voltage (V), current (I) and the thickness of oil film (h), the pitting area can be expressed as [90]:

$$A_p = 0.081h^{0.116}V^{0.289}I^{1.179}.$$

This equation confirms the key role of the current.

3.1.3 *Fluting*

As a result of the periodic currents, fluting is the most common damage, manifested as flute burnt scars evenly distributed along the circumference of the bearing race. Under the microscope, a fluting pattern occurs like a washboard with ''dark stripes'' and ''bright stripes'' (Fig. 7(a)). However, under scanning electron microscopy (Fig. 7(b)), the fluting pattern is composed of scratch marks [91]. Prashad et al. studied the relationship between the resistance of the contact area and the damage mode, and they found that low-resistance contacts caused electrochemical decomposition/corrosion of grease and gradually

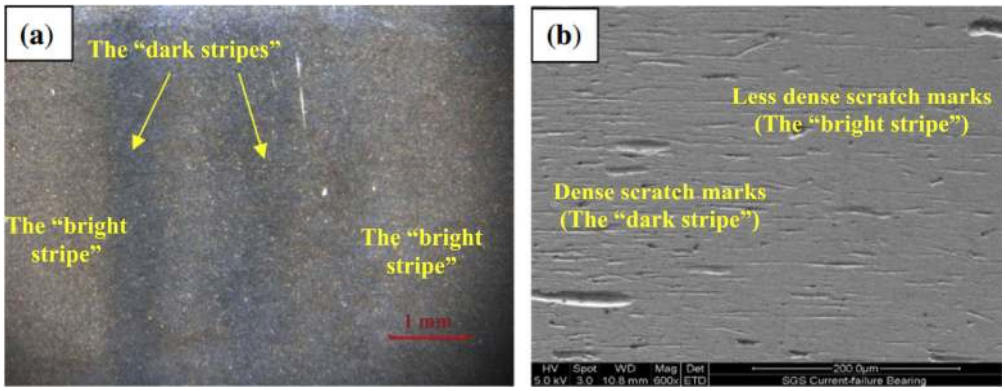

Fig. 7 Characterizations of the fluting patterns. (a) Stereomicroscope. (b) Scanning electron microscopy. Reproduced with permission from Ref. [91], © Elsevier 2014.

leaded to fluting, while high-resistance contacts were more likely to induce pitting [92]. By analyzing the fluting surface and wear debris, Liu et al. suggested that the nature of fluting was a three-body abrasive wear caused by the vibration of bearing rollers, while the vibration was excited by the bearing current [91]. This dual effect of mechanical and electrical discharge can also explain the appearance of fluting in heavy-load areas. In addition, fluting is also a critical stage in bearing tests.

3.1.4 *Spark tracks*

The initial appearances of spark tracks are irregular scratches askew to the direction of rotation (Fig. 8). Although looking like a mechanical scratch, the spark track also has an electric nature. The bottom of the track is sometimes melted, and the corners of the scratch are sharp, which should be more rounded as a result of mechanical scraping [32]. In addition, the depth of a spark track is consistent with its entire surface. The cause for the spark tracks is proposed as the debris blasted out of the surface by electrical discharges.

3.1.5 *Welding*

Welding mainly occurs in the housing splits, pads and seals of the bearing, and it is attributed to the thermal effect when a large amount of current passes the bearing (Fig. 9) [32]. However, as discussed in the previous section, the usual EDM process cannot generate such a large current flow, and hence welding is mainly caused by direct momentary contact between the stator and the rotor. This phenomenon has characteristics such as spot welding that can be easily distinguished.

According to different working parameters, such as load, rotate speed, bearing type, roller and interface material, and lubricant conductivity, the appearance of electrical damages varies widely. Didenko and

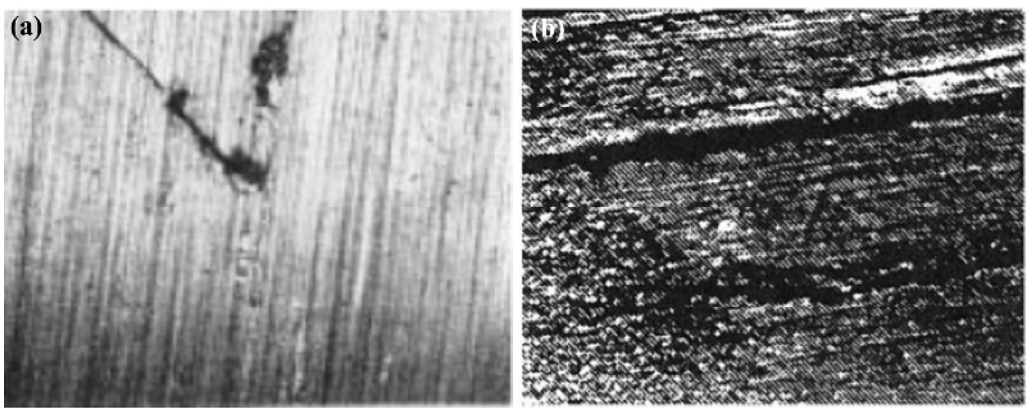

Fig. 8 (a) Molten spark tracks. Reproduced with permission from Ref. [93], © IEEE 2000. (b) 60 times magnification of a spark track. Reproduced with permission from Ref. [85], © IEEE 1991.

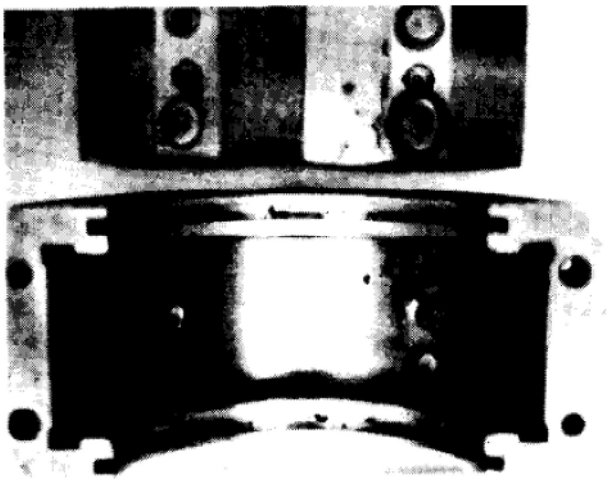

Fig. 9 The most severe case of electrical bearing failure: welding. The pads were welded into its retainer. Reproduced with permission from Ref. [85], © IEEE 1991.

Pridemore observed a different fluting pattern in the roller, in comparison with the outer race of a Tri-Lobe roller bearing [94]. As shown in Fig. 10, the anode (roller) has wider and shallower "craters", while the cathode has narrower and deeper ones. Using an electrical pitting wear tester, Raadnui et al. provided a corrugated parameter model, containing load, current, housing temperature and test duration [95]. As for the pitting wear debris, long test duration and a large current will enhance the production of black spherical wear particles. In the case of weak bearing currents of no more than ~mA, Xie et al. found pitting marks on the inner ring using a lubricant with a higher conductivity than an insulated lubricant [96].

3.2 Lubrication failures

In addition to the morphological damage, lubrication failure under charged conditions is also a key issue that has attracted a lot of attention in recent years [97, 98]. Improper lubrication can lead to increased friction and wear, unstable operation, resulting in a sharp reduction of bearing lifetime [45].

3.2.1 *Degradation of lubricant*

In a bearing, the lubricant should be capable to reduce friction and wear, evacuate the heat, inhibit corrosion, and clean the surface, etc. [99–101]. In a well-lubricated running bearing, the two counterfaces are completely separated by a thin lubricant film, avoiding direct contact. Therefore, the traditional mode of bearing failure mode can be improved by suitable lubrication strategies. Although lubricants are generally chemically inert, shaft voltage and bearing current provide the potential and energy required for chemical reactions, accelerating the degradation process [102]. The free radicals generated by electrical excitation will rapidly react with oxygen to form peroxide groups, which in turn induce the formation of new radical groups, and such a chain reaction will eventually form carboxyl-containing products [82]. Commonly, there will be oxidation of base oils, antioxidants, and thickeners, which will produce acidic and highly viscous products, resulting in the loss of lubricity. Along with this process, lubricating additives in the lubricant, such as molybdenum disulfide, are found to be separated from the lubricant and agglomerated onto the raceway, and these lubricants additives also degrade with the application of an electric field [103, 104]. Moreover, the thermal effect of the discharge process would also cause the evaporation of the oil component, which was considered as the main factor for the grease failure in

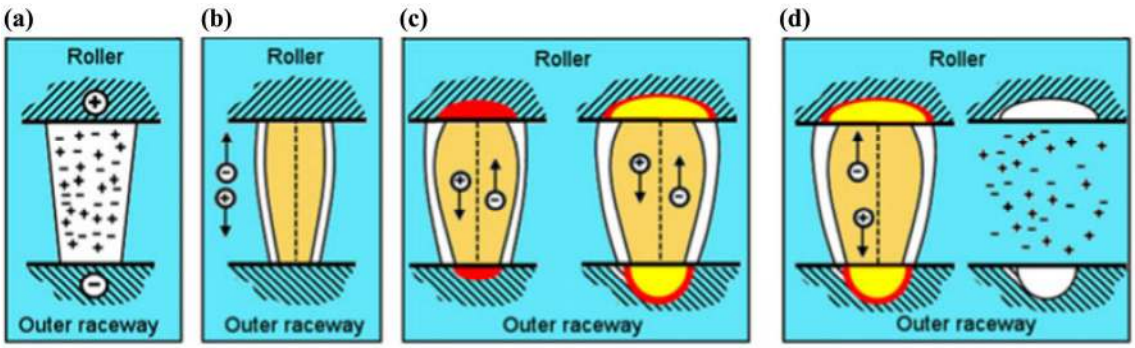

Fig. 10 Electrical discharge process between the roller and the outer raceway of the bearing. (a) Ignition. (b) Path formation. (c) Discharging. (d) Ejection. Reproduced with permission from Ref. [94], © Springer Nature 2012.

cylindrical roller bearings [105].

3.2.2 *Microbubble effects*

The generation of microbubbles in charged lubricant films was first discovered by Luo et al. with the relative optical interference intensity technique [106]. Under charged condition, abundant microbubbles appeared around the lubricated contact area (Fig. 11), which was proposed to be attributed to local overheating [83, 107]. Correspondingly, when moving to the outer region, the bubble tended to be unstable and the coalescence sometimes occurred (Fig. 11). The generation and collapse of microbubbles can destabilize the lubrication, which can lead to additional noise and vibration in a bearing [107]. In addition, lubricants containing microbubbles are more susceptible to electrical breakdown. An anomalous phenomenon is that the generation of microbubbles was more intense after the electrode was coated with an insulating layer, and the required input electrical energy was much smaller compared with that of the uncoated electrode [108]. The bubble generation was also found to be closely related to the frequency of the AC electric field. Similarly, the difference in the threshold voltage and current caused by the frequency was also enhanced by the interfacial dielectric properties. Based on a series of experimental and theoretical studies, a detailed model containing the formation and motion of microbubbles in nanoconfined liquid films was established [109]: As a result of competition for the microbubble generation and the liquid refilling, large bubbles appeared in the lubricants with a high surface tension or a high liquid viscosity. In terms of motion, microbubbles were driven by the pressure gradient in the contact zone, dielectrophoresis force and viscous drag.

3.2.3 *Interfacial stress induced by electric field: Electrowetting*

The contact angle of a droplet on a surface can be regulated by a voltage between the electrodes, which is called the electrowetting effect [110]. This electromechanical mechanism dominates the microfluidic behavior by modifying the interfacial tension [111]. More relevant to the bearing working conditions, it is observed that the nonpolar dielectric lubricant in the contact area of a steel ball and a metallic layer will spread along the surface under the action of an electric field [112]. In the case of emulsion, a typical two-phase immiscible liquid system used as the lubricant, the stable dispersion state of the two-phase system would be destroyed by the electrostatic pressure and the surface tension due to the difference in dielectric properties [113–115]. Thus, the lubrication properties could be unstable due to the coalescence of emulsion droplets. Adopting a simplified needle-plate barrier discharge experiment, Lee et al. investigated the effect of discharges on lubrication stability [116]. A deformation of an oil film was observed under a high voltage, and a surface fluctuation occurred when the voltage was switched. Furthermore, this deformation was related to the voltage polarity and the temperature, and the negative voltage polarity and the high temperature helped to deform for silicone oil droplets [117].

In addition to the lubrication failure modes mentioned above, the shaft voltage and bearing current also have some other effects. For instance, the interfacial electric field enhances the electrostatic interaction between the rollers and the raceway, generating extra electrostatic pressure. Moreover, a reduction in the lubricant flow of a confined liquid film was also observed under an electric field [118].

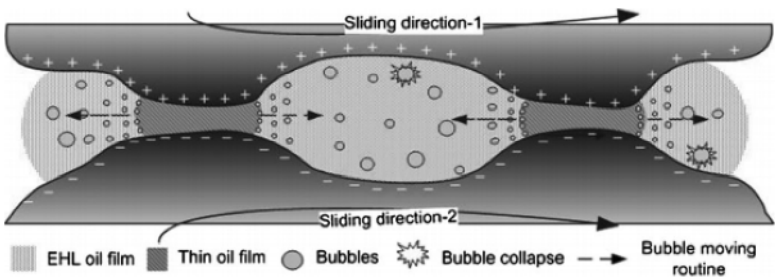

Fig. 11 Schematic diagram of the microbubble generation and motion in the elastohydrodynamic lubrication (EHL) oil film under charged condition. Reproduced with permission from Ref. [107], © AIP Publishing 2008.

4 Fundamental researches on tribological performance in an electrical environment

As mentioned above, the presence of shaft voltage and bearing current has brought out an urgent need to improve the lubrication state of the bearing. In a properly designed lubrication system, morphological damages and lubrication failures caused by the electrical environment can be weakened or eliminated [119, 120]. In order to achieve the suppression of electrical damage and even use the electrical environment to promote lubrication, an in-depth understanding of the relationship between the lubrication properties and the electric field/current/charges is needed [121].

In the past decades, researchers have made great efforts to promote fundamental researches on the tribological performance in an electrical environment. The electrical failure is decomposed into several scientific subjects concerning the effect of electric field on friction and wear, in which lots of remarkable results revealing the underlying physical and chemical nature have been demonstrated. These results help to fill the blank in the theory of lubrication under charged conditions, as well as provide guidance for the design of lubrication systems in practice. It has been confirmed by a large number of experiments that the lubrication/friction properties can be tuned by an external electric field [122–124]. However, unlike specific electrical damages that have common appearances, the electrical responses of the lubrication properties are significantly different, and multiple mechanisms are involved. As shown in Fig. 12, there have been four main influence mechanisms of the effects of the electric field/charge on the lubrication performances so far [125–130]: (1) electrostatic interaction; (2) structural change/transfer film formation; (3) changes in physical/chemical properties; (4) carrier/charge distribution. In actual situations, these mechanisms are often used collectively, while their contributions vary in different material systems and under different working conditions.

4.1 Electrostatic interaction

Electrostatic interactions are common at all frictional interfaces, and the classification here refers only to the category of the electrostatic forces acting directly on the friction interaction. The stronger the electrostatic interaction, the more severe the friction and wear. Weaker electrostatic interaction promotes lubrication.

Firstly, due to the difference in the Fermi levels of different materials, electron transfer occurs when dissimilar materials contact, to reach a balance of the potential at the interface, thereby generating the contact potential (i.e., self-generated potential) [131]. As a result, the positive and negative charge centers are formed on both sides of the interface, giving rise to the electrostatic force at the interfaces. In addition, the surface static charges and the transient polarization charges formed by the triboelectric effect further enhance the electrostatic interaction. By offsetting the self-generated potential by the application of an external electric field, Yamamoto et al. achieved the friction reduction [132]. The friction forces of 34 kinds of metallic friction pairs in open circuit, short circuit, zero current (i.e., the external voltage offsets the self-generated potential), and constant current (forward and reverse) conditions were compared by Chen et al. [133, 134]. It was found that for the Fe, Co, Ni, Ti, Cr and Cu systems, the friction forces in the open circuit state and the zero current state were smaller than those in other electrical states, and the friction at zero current was the lowest [133, 134]. Conversely, it is also possible to strengthen the charge separation at the interface by an external electric field. Further, the friction and wear mechanism of the stainless steel changes with interfacial potential differences, and it is proposed that adhesive wear dominated under the low potential difference and abrasive wear dominated under the high potential difference[135]. Thus, it was believed that slightly increasing the interfacial potential difference during the running-in phase could effectively shorten the running-in period, while in other friction stages, it was necessary to reduce the potential difference reasonably to reduce friction and wear. The applied electric field not only affects the conductor/conductor friction pair, but also applies to any metal-containing friction pair. The electric filed between carbon black rubber and aluminum to cause the electrostatic attraction between the contact peaks was energized by Hurricksa, and a significant friction

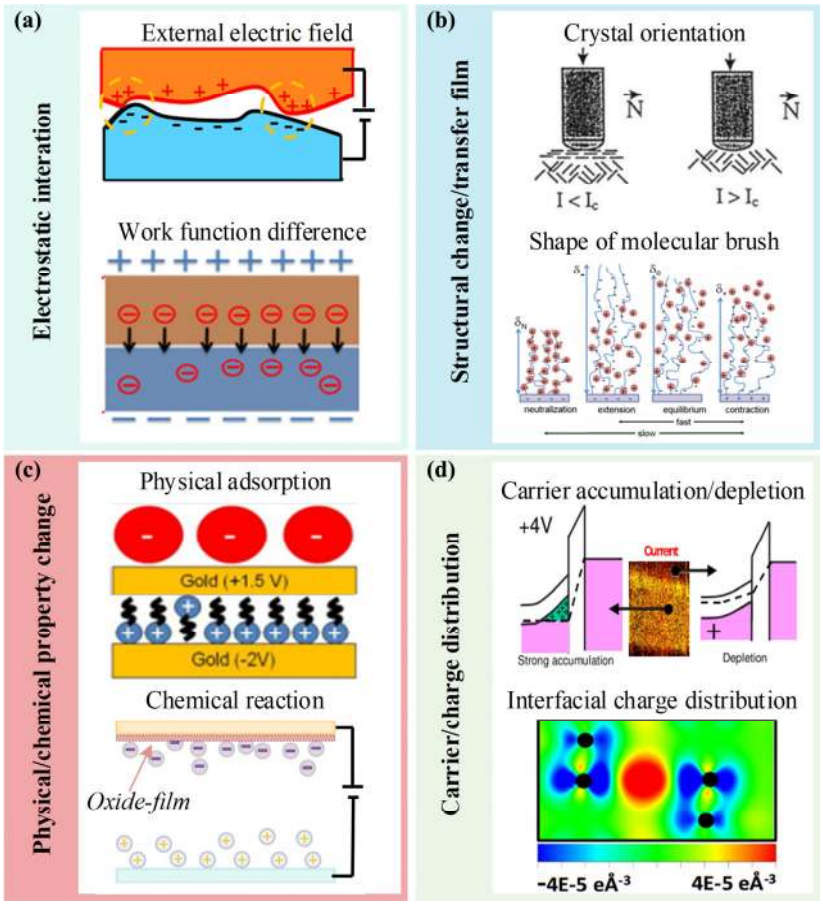

Fig. 12 Influences of the electric field/charge on the lubrication performance. (a) Electrostatic interaction induced by an external electric field and work function difference. (b) Structural change/transfer film: High current changes the crystal orientation of the transfer film. Reproduced with permission from Ref. [125], © Elsevier 1999. The electric field changes the shape of the molecular brush (from compression to stretching). Reproduced with permission from Ref. [126], © American Physical Society 2012. (c) Physical/chemical property change: Surface potential affects the type of physically adsorbed ions (reproduced with permission from Ref. [127], © American Physical Society 2012), as well as induces chemical reaction at the anode. (d) The rearrangement of carrier/charge distribution under the electric field: carrier accumulation/depletion. Reproduced with permission from Ref. [129], © American Physical Society 2007; interfacial charge distribution. Reproduced with permission from Ref. [130], © Springer Nature 2015.

increase was observed [136]. Similarly, the applied electric field can also enhance the friction in the stainless steel/ice [137, 138], ferroelectric materials/stainless steel [139, 140] systems.

In the micro/nanoscale friction experiments on the basis of atomic force microscopy, the interfacial adhesion force can also be effectively tuned by applying an electric field between the AFM tip and the sample surface. However, so far, the researches on molybdenum disulfide [141], InAs nanowires [142], and silicon/silicon dioxide materials [143, 144] have generally suggested that the electric field enhanced friction and wear. It is worth mentioning that Liu et al. studied the friction response of the Langmuir–Blodgett monolayer films under the actions of a DC voltage and an AC voltage [145]. It was found that the DC voltage enhanced friction, while a friction reduction was observed under an AC voltage of certain frequencies, owing to the vibration effect of the fluctuating electrostatic force [145].

4.2 Structural change/transfer film formation

The structural change/transfer film formation mechanism is mainly embodied in the friction pair containing an interfacial structure with electrical responsiveness. With the application and removal of the interfacial electric field, the contact surface exhibits different molecular structures or transfer film

orientations, corresponding to different lubrication properties.

In the case of dry friction, Csapo et al. studied the dynamic electrical contact friction behavior of graphite-graphite under argon atmosphere, and found that the friction coefficient increased significantly after applying a current [146]: Specifically, the graphite particle crystals at the contact position recombined, so that the basal plane was parallel to the sliding surface, resulting in a decrease in the friction coefficient. When the current passed, the basal plane of the graphite particles was transformed to be perpendicular to the sliding surface to enhance the interfacial conductivity. This change increased the contact points per unit area, enhancing friction and wear. In the controlled atmosphere, the graphite-graphite and graphite-copper friction pairs showed reduced friction and increased wear under the passage of the current owing to the formation of the oxidative transfer film.

Lavielle et al. studied the friction between ternary polyethylene film (pin) and steel (disc) under different electrical conditions [147]: when a forward voltage was applied, the carboxyl group on the polymer surface was repelled by the steel surface, which mainly showed the lubrication of the alkyl group; when a reverse voltage was used, the adhesion of the carboxyl group to the steel surface was enhanced to increase the friction. Similarly, the friction properties of graphene oxide [148] and self-assembled monolayer [149] also differed under forward and reverse voltages.

Such a mechanism is more widely used in liquid environments. Sweeney et al. achieved the control of the surface adsorption state by controlling the potential of the gold surface in the perchlorate/sulphate solution, and thereby controlling the lubrication properties of the surface [127]. Herminghaus et al. controlled the lubrication performance and the bearing capacity by controlling the molecular brush shape of the polymer electrolyte through the potential [150]. Similar studies have expanded to more liquid-phase environmental systems in recent years, such as long-chain alkanes [151], polyols [152], various ionic liquids [153, 154] and hydrogels [155].

The structural change/transfer film formation mechanism can achieve two-way (enhancing and weakening) lubrication performance control, because it can control the interface morphology, and it is easier to achieve lubrication than other mechanisms.

4.3 Changes in physical/chemical properties

As compared with the former mechanisms, this influence mechanism mainly emphasizes the chemical reaction and the physical absorption at the interface. With the application of an electric field, polar molecules, anions and cations in the lubricant will be physically adsorbed to the charged interfaces. Chemical reactions occur on the contact surfaces when the external electric potential meets the electromotive force (EMF). These effects change the physical/chemical properties of the original surface and thus change its frictional properties.

For water-based lubricants or organic lubricants with reactive functional groups, discharges induce the hydroxide or reactive groups to accumulate on the metal surface. The representative work is a series of metal/ceramic friction pairs developed by Meng et al., and they found that the applied voltage increased the friction, because the hydroxide ions formed by the water decomposition at the metal electrode aggregated and reacted with the metallic surface to form a phase film [124, 156]. Zhai et al. found that the saponification reaction of GCr15/45 interface in the aluminum stearate solution was varied by the applied voltage, and different adsorption characteristics of the saponified film corresponded to different friction properties [157].

For dry friction, Paulmier et al. explored the friction properties of the graphite/XC48 carbon steel friction pair under the passage of the current [158]. It was found that the steel surface formed an oxide film after the application of the current in the atmosphere, and the friction was reduced by 35% when the steel was the cathode. Moreover, similar effects could apply to the graphite/copper [159], graphite/graphite [160], and CN_x film/aluminum [161] friction pairs in the atmosphere.

4.4 Carrier/charge distribution

In terms of the frictional energy dissipation process, the electronic excitations and creation of electron-hole pairs enhance the energy loss. The rearrangement of carrier/charge distribution under the electric field

could influence these processes, leading to the changes in friction.

A systematic study on silicon pn junctions was carried out by Park et al., and it was revealed the feasibility of electronically controlled friction [129, 162]: As compared to the n region, the p region shows a higher friction force under the external electric field. It was proposed by the authors that the strong accumulation of carriers in the p region produced a large ohmic loss and increased the friction. By applying an external electric field, Wang et al. regulated the charge distribution between graphene layers and tuned the interlayer friction [130]. In addition, the stress in the contact region could produce a series of changes in the electrical property change: the induced bending and carrier dispersion affected the interface dislocation mobility, and the formation of local quantum dots in the contact region promoted the electron-hole pair recombination.

In Fig. 13, the detailed material systems in the fundamental researches and the proportion that each mechanism works are summarized. It can be concluded that the electric field can be used to tune the lubrication performances. Particularly, the use of polar lubricants or additives in the liquid phase can effectively maintain the lubrication performance under charged conditions. However, more efforts need to be made to bring these experimental results to industrial applications.

5 Solutions to electrical bearing failures

The purpose of studying electrical failure is to prolong the bearing service life and achieve long-term stability. In the following part, some effective solutions to the electrical bearing failures will be discussed in the following part.

5.1 Reasonable grounding and minimizing the electric field

A typical patented solution is the use of a grounding ring composed of conductive microfibers, which is installed on the shaft outside the bearing [163]. With the conductive brushes connected to the shaft, the ground ring works as a diverter, directing the shaft voltage to ground and bypassing currents that would otherwise flow through the bearing (Fig. 14) [164, 165]. It has been proven that this technique works well for the EDM currents and the high-frequency circulating currents.

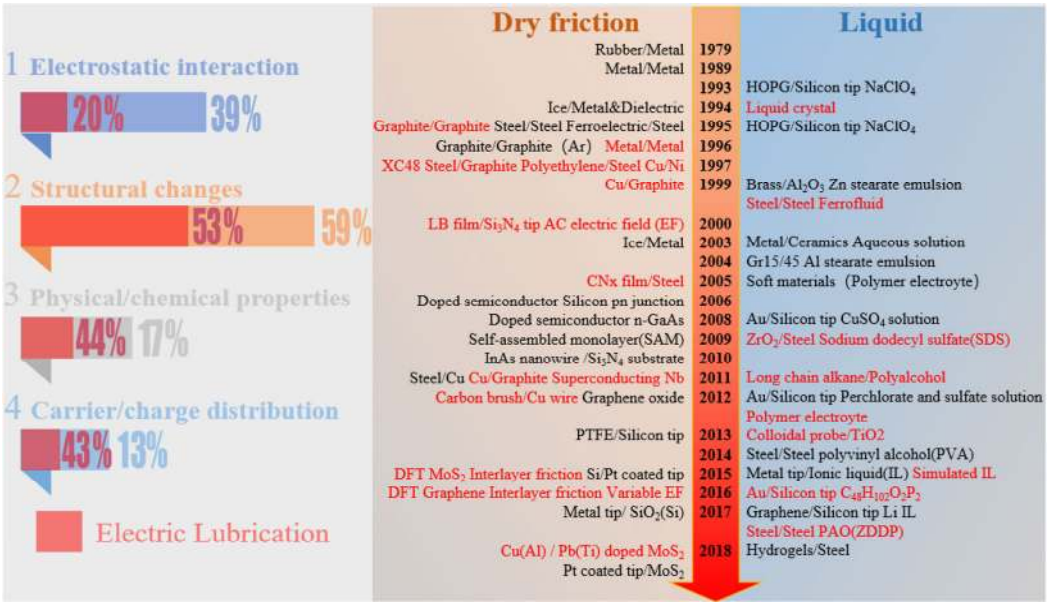

Fig. 13 The material systems in the researches on the relationship between the electric field and the lubrication properties. The percentages represent the proportion of different mechanisms involved in literature: 39% of the studies involve electrostatic interactions, 59% of the studies involve structural changes, 17% of the studies involve physical/chemical properties change, and 13% of the studies involve carrier/charge distribution. The red parts represent the proportion of the lubrication effect in each mechanism, the corresponding material systems are also marked red.

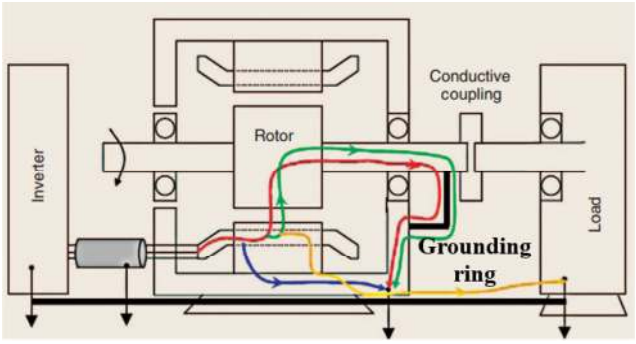

Fig. 14 Schematic diagram of an electric motor using a ground ring. Reproduced with permission from Ref. [163], © IEEE 2004.

One reasonable idea is to suppress CMV from the source. Simply reducing the switching frequency of the inverter can reduce the electrical damages, and however, it will limit the performance of the speed control system. An active approach is to add CMV filters between the inverter and the motor [166]. This method will divert the CMV away from the motor, and the currents will be directed back to the inverter or to the ground [167]. The filter design has been well developed in recent years. Pairodamonchai et al. suggested a hybrid output EMI filter to eliminate the high-frequency CMV components [168], and the researches on the optimization of filters have also been reported [169, 170]. Moreover, an advanced inverter design can also help to reduce CMV: The active zero state PWM (AZSPWM) method [171] and the near state PWM (NSPWM) method [172] effectively suppress the neutral voltage of a motor.

Another strategy is to shield the electric field [173]. Busse et al. evaluated a modified induction motor, i.e., electrostatic shielded induction motor, and the PWM induced shaft voltages could be effectively suppressed by constructing a Faraday shield in the air gap between the stator and the rotor [174]. Similarly, by shielding the wires between the inverter and the motor, the capacitively coupled current was effectively weakened [175].

5.2 Suppress the electrical breakdown

5.2.1 Improve the insulation performance of the bearing

A classic way to suppress the high-frequency bearing current is to build an insulation layer on the bearing [176, 177]. For example, hybrid/full ceramic bearings have been used in commercial EV [51]. The purpose of this method is to raise the impedance between the bearings and the ground. Thereby, electric discharges can be prevented by the insulating layer. Circulating currents can be significantly suppressed by the ceramic or hybrid bearings, while the EDM currents are less affected [178]. However, an insulated bearing limits the dissipation of the heat flow from the rotor. Furthermore, the insulation method sometimes transforms the discharge process and changes the proportion of the different components of the currents. Therefore, enough attention should be paid to the current composition.

5.2.2 Enhance the conductivity of the lubricated interface

In contrast, the solution on the basis of enhanced conductivity also works in some systems. Although it seems to be the opposite of the insulating methods, it has been experimentally proved that a conductive grease can prevent the fluting [88]. Suzumura suggested that due to the formation of electrical channels, the electric current density of the rolling contact area with conductive greases was lower than that with non-conductive greases [88]. In terms of energy consumption, the insulated interfaces can be easily corroded during discharging when a large amount of energy is released instantaneously in a confined area, and the interfaces with an excellent conductivity accumulate less energy. Therefore, suppressing the interfacial resistance, which is related to nonconducting lubricants, insulating surface layers and asperity contacts, could be effective [179]. However, the method is closely related to the lubricant components, and simply adding metal particles to the grease could increase mechanical wear [180]. Thereby, a well-designed electric contact lubricant is required to ensure the lifetime and reliability of the system. Zhang et al. added carbon black into traditional overbased calcium sulfonate complex grease and lithium, enhancing their conductivity, friction-reduction and anti-wear properties [181]. Conductive greases based on lithium salts ($LiBF_4$, $LiPF_6$, $LiNTf_2$) and their related ionic liquids also showed excellent lubrication properties. Typically, the use of ionic liquids, which are composed of weakly coordinated anions and organic cations, has attracted a lot of interest. In addition to the characteristics satisfying the needs of a lubricant, e.g., non-volatile, non-flammable, and low melting point,

the dipolar structure of ionic liquids (ILs) helps form a boundary lubricant film, and meanwhile, the high conductivity suppresses arc discharges [120].

Transition metal powders (gold, silver and copper) provide excellent electric conductivities, and however their lubrication properties and resistance to degradation are poor [182]. Thus, these materials have been used as the surface or coating materials in the form of functional composites, e.g., $AgSnO_2$, AgI, Ag/C, CuW, Cu/C, carbon nanotube film and graphene [183–187]. However, there is still a lack of long-life industrial lubricants with outstanding interfacial conductivities and desirable lubricities. The use of additives such as silver is too expensive for industrial applications, and some ILs are corrosive. In addition, this method only weakens the effect of the current, which does not avoid the influence of the electrical environment. A large number of new materials are still in the experimental stage. To meet the high-speed, high-load, complex vibration conditions and achieve commercialized mass production, great efforts need to be made.

In conclusion, because different inverter-motor systems induce different bearing currents, specific strategies can vary dramatically. Some technologies such as voltage filters, although effective, are not suitable for industrial uses because of their high costs and difficulty in installation.

6 Summary and outlook

The researches on the premature electrical failure of bearings are one of the key bottlenecks in electric vehicles at present and in the forthcoming decades. In this paper, an overview on electrical bearing failure in electric vehicles has been presented. Relevant topics such as common mode voltages, bearing currents, electric discharge machining and lubrication instability have been regrouped to get a comprehensive and systematic perspective on the phenomena. The generation and composition of shaft voltage and bearing current and the appearance of electrical bearing failure, and then to fundamental researches on lubrication behaviors under charged conditions, and finally feasible ways to solve the problem, are discussed. In terms of the depth and breadth of current studies, considerable efforts have been made to classify and quantify bearing voltages and currents, and however the lurking lubrication problems have received less attention. Nevertheless, the recent progress of fundamental lubrication researches has continuously improved the theoretical systems of the lubrication behaviors under charged conditions, which could guide the design and the protection of electrical contact interfaces.

Based on this study, more researches on relevant directions are still urgently needed, which are enumerated below:

(1) A commonly used bearing current prediction model for various motor systems is still lacking. This paper reviews the most typical shaft voltage and bearing current modes of the induction motors. However, the motor and inverter control systems of different electric vehicles are not completely consistent, and the design of the overall electrical system, as well as the type of the motor, can vary greatly. For instance, in an electric vehicle driven by wheel-hub motors, the compositions of shaft voltages and bearing currents are more complicated. More work is needed to detect, classify and quantify the electrical environments in these systems.

(2) A bridge is needed to closely relate the study of the lubrication failure under charged conditions to the actual bearing failures. Although many fundamental mechanisms have been revealed, the electrical environment in which the bearing actually works is much more complicated than that in the experiment, and how these mechanisms correlate with each other is still an open question. Furthermore, the electrical failure of bearings is mainly studied on the basis of the damage morphology. The running state of the bearing (e.g., lubrication instability) will be potential and compelling directions.

(3) More comprehensive, flexible, low-cost solutions that can meet industrial needs are desirable. The foregoing parts have summarized several strategies to suppress the electrical bearing failures, and while turning these technologies into industrial applications is still challenging. Recent development of new materials offers a broader range of possible solutions, e.g., self-lubricating and self-healing materials, smart surface structures with electrical responses. Hence,

exploring the application of new lubricating materials in motor bearings could be an integrated part of future researches.

Acknowledgements

This work was supported by the National Natural Science Foundation of China (Grant Nos. 51822505 and 51527901), Tsinghua University Initiative Scientific Research Program (Grant No. 2019Z08QCX11), and Beijing Natural Science Foundation of China (Grant No. 3182010).

References

[1] Larminie J, Lowry J. *Electric Vehicle Technology Explained. 2nd ed*. Hoboken (USA): John Wiley & Sons, 2012.

[2] Patil P G. Prospects for electric vehicles. *IEEE Aerosp Electro Syst Mag* **5**(12): 15–19 (1990)

[3] Safari M. Battery electric vehicles: Looking behind to move forward. *Energy Policy* **115**: 54–65 (2018)

[4] Amjad S, Neelakrishnan S, Rudramoorthy R. Review of design considerations and technological challenges for successful development and deployment of plug-in hybrid electric vehicles. *Renew Sustain Energy Rev* **14**(3): 1104–1110 (2010)

[5] Darabi Z, Ferdowsi M. Aggregated impact of plug-in hybrid electric vehicles on electricity demand profile. *IEEE Trans Sustain Energy* **2**(4): 501–508 (2011)

[6] Apfel D C. Exploring divestment as a strategy for change: An evaluation of the history, success, and challenges of fossil fuel divestment. *Soc Res* (4): 913–937 (2015)

[7] Miller R G. Future oil supply: The changing stance of the international energy agency. *Energy Policy* **39**(3): 1569–1574 (2011)

[8] Popa M E, Vollmer M K, Jordan A, Brand W A, Pathirana S L, Rothe M, Röckmann T. Vehicle emissions of greenhouse gases and related tracers from a tunnel study: CO: CO_2, N_2O: CO_2, CH_4: CO_2, O_2: CO_2 ratios, and the stable isotopes 13C and 18O in CO_2 and CO. *Atmos Chem Phys* **14**(4): 2105–2123 (2014)

[9] Pelletier S, Jabali O, Laporte G. Goods distribution with electric vehicles: Review and research perspectives. *Transp Sci* **50**(1): 3–22 (2016)

[10] Tseng H K, Wu J S, Liu X S. Affordability of electric vehicles for a sustainable transport system: An economic and environmental analysis. *Energy Policy* **61**: 441–447 (2013)

[11] Tran M, Banister D, Bishop J D K, McCulloch M D. Realizing the electric-vehicle revolution. *Nat Climate Change* **2**(5): 328–333 (2012)

[12] Kumar M S, Revankar S T. Development scheme and key technology of an electric vehicle: An overview. *Renew Sustain Energy Rev* **70**: 1266–1285 (2017)

[13] Yong J Y, Ramachandaramurthy V K, Tan K M, Mithulananthan N. A review on the state-of-the-art technologies of electric vehicle, its impacts and prospects. *Renew Sustain Energy Rev* **49**: 365–385 (2015)

[14] Paplicki P, Piotuch R. Improved control system of PM machine with extended field control capability for EV drive. In *Mechatronics—Ideas for Industrial Application*. Awrejcewicz J, Szewczyk R, Trojnacki M, Kaliczyńska M, Eds. Cham: Springer, 2015: 125–132.

[15] Habib S, Khan M M, Abbas F, Sang L, Shahid M U, Tang H J. A comprehensive study of implemented international standards, technical challenges, impacts and prospects for electric vehicles. *IEEE Access* **6**: 13866–13890 (2018)

[16] Rind S, Ren Y X, Jiang L. Traction motors and speed estimation techniques for sensorless control of electric vehicles: A review. In *Proceedings of 2014 49th International Universities Power Engineering Conference*, Cluj-Napoca, Romania, 2014: 1–6.

[17] Williamson S S. EV and PHEV battery technologies. In *Energy Management Strategies for Electric and Plug-in Hybrid Electric Vehicles*. Williamson S S, Ed. New York: Springer, 2013: 65–90.

[18] Esteban B, Sid-Ahmed M, Kar N C. A comparative study of power supply architectures in wireless EV charging systems. *IEEE Trans Power Electron* **30**(11): 6408–6422 (2015)

[19] Teixeira A C R, Da Silva D L, Machado Neto L D V B, Diniz A S A C, Sodré J R. A review on electric vehicles and their interaction with smart grids: The case of Brazil. *Clean Technol Environ Policy* **17**(4): 841–857 (2015)

[20] Li S J, Tong L, Xing J W, Zhou Y Y. The market for electric vehicles: Indirect network effects and policy design. *J Assoc Environ Resour Economists* **4**(1): 89–133 (2017)

[21] Babrowski S, Heinrichs H, Jochem P, Fichtner W. Load shift potential of electric vehicles in Europe. *J Power Sources* **255**: 283–293 (2014)

[22] Chan C C. An overview of electric vehicle technology. *Proc IEEE* **81**(9): 1202–1213 (1993)

[23] Chan C C, Bouscayrol A, Chen K Y. Electric, hybrid, and fuel-cell vehicles: Architectures and modeling. *IEEE Trans Veh Technol* **59**(2): 589–598 (2010)

[24] Doerr J, Ardey N, Mendl G, Fröhlich G, Straßer R, Laudenbach T. The new full electric drivetrain of the Audi e-tron. In *Der Antrieb von morgen 2019*. Johannes L, Ed. Wiesbaden: Springer Vieweg, 2019: 13–37.

[25] Jelden H, Pelz N, Haußmann H, Kloft M. The plug-in hybrid drive of the VW passat GTE. *MTZ Worldwide* **76**(9): 16–23 (2015)

[26] Cheng K W E. Recent development on *electric vehicles. In Proceedings of 2009 3rd International Conference on Power Electronics Systems and Applications*, Hong Kong, China, 2009: 1–5.

[27] Yildirim M, Polat M, Kürüm H. A survey on comparison of electric motor types and drives used for electric vehicles. In *Proceedings of 2014 16th International Power Electronics and Motion Control Conference and Exposition*, Antalya, Turkey, 2014: 218–223.

[28] Boztas G, Yildirim M, Aydogmus O. Design and analysis of multi-phase BLDC motors for electric vehicles. *Eng Technol Appl Sci Res* **8**(3): 2646–2650 (2018)

[29] Nam K H. *AC Motor Control and Electrical Vehicle Applications*. *2nd ed.* Boca Raton (USA): CRC press, 2018.

[30] Chun Y D, Park B G, Kim D J, Choi J H, Han P W, Um S. Development and performance investigation on a 60kW induction motor for EV propulsion. *J Electr Eng Technol* **11**(3): 639–643 (2016)

[31] Alger P L, Samson H W. Shaft currents in electric machines. *Trans Am Inst Electr Eng* **43**: 235–245 (1924)

[32] Costello M J. Shaft voltages and rotating machinery. *IEEE Trans Ind Appl* **29**(2): 419–426 (1993)

[33] Erdman J M, Kerkman R J, Schlegel D W, Skibinski G L. Effect of PWM inverters on AC motor bearing currents and shaft voltages. *IEEE Trans Ind Appl* **32**(2): 250–259 (1996)

[34] Busse D, Erdman J, Kerkman R J, Schlegel D, Skibinski G. Bearing currents and their relationship to PWM drives. *IEEE Trans Power Electron* **12**(2): 243–252 (1997)

[35] Kim B T, Koo D H, Hong J P, Kwon B I, Jun J H. A study on analysis of inverter-fed induction Motor's bearing current using improved equivalent ciruit parameters. *Trans Korean Inst Electr Eng* **56**(4): 683–692 (2007)

[36] Jones R W, Seaver D E. Investigation and results of eddy currents on DC motor bearings. In *Proceedings of Annual Technical Conference on Pulp and Paper Industry*, Seattle, WA, USA, 1990: 145–150.

[37] Nippes P I. Early warning of developing problems in rotating machinery as provided by monitoring shaft voltages and grounding currents. *IEEE Trans Energy Convers* **19**(2): 340–345 (2004)

[38] Mukherjee R, Patra A, Banerjee S. Impact of a frequency modulated pulsewidth modulation (PWM) switching converter on the input power system quality. *IEEE Trans Power Electron* **25**(6): 1450–1459 (2010)

[39] Ahola J, Särkimäki V, Muetze A, Tamminen J. Radio-frequency-based detection of electrical discharge machining bearing currents. *IET Electr Power Appl* **5**(4): 386–392 (2011)

[40] Zhang P J, Du Y, Habetler T G, Lu B. A survey of condition monitoring and protection methods for medium-voltage induction motors. *IEEE Trans Ind Appl* **47**(1): 34–46 (2011)

[41] Singh G K, Ahmed Saleh Al Kazzaz S. Induction machine drive condition monitoring and diagnostic research—A survey. *Electr Power Syst Res* **64**(2): 145–158 (2003)

[42] Lawson J A. Motor bearing fluting. In *Proceedings of Conference Record of 1993 Annual Pulp and Paper Industry Technical Conference*, Hyannis, MA, USA, 1993: 32–35.

[43] Boyanton H E, Hodges G. Bearing fluting [motors]. *IEEE Ind Appl Mag* **8**(5): 53–57 (2002)

[44] Boškoski P, Petrovčič J, Musizza B, Juričić Đ. Detection of lubrication starved bearings in electrical motors by means of vibration analysis. *Tribol Int* **43**(9): 1683–1692 (2010)

[45] Walther H C, Holub R A. Lubrication of electric motors as defined by IEEE standard 841-2009, shortcomings and potential improvement opportunities. In *Proceedings of 2014 IEEE Petroleum and Chemical Industry Technical Conference*, San Francisco, CA, USA, 2014: 91–98.

[46] Ost W, De Baets P. Failure analysis of the deep groove ball bearings of an electric motor. *Eng Fail Anal* **12**(5): 772–783 (2005)

[47] Shami U T, Akagi H. Identification and discussion of the origin of a shaft end-to-end voltage in an inverter-driven motor. *IEEE Trans Power Electron* **25**(6): 1615–1625 (2010)

[48] Fiser R, Ferkolj S. Magnetic field analysis of induction motor with rotor faults. *COMPEL - Int J Comput Math Electr Electron Eng* **17**(2): 206–211 (1998)

[49] Asakura Y, Akagi H. Mechanism of shaft end-to-end voltage generation by asymmetry in an inverter-driven motor. *IEEJ Trans Ind Appl* **132**(3): 404–410 (2012)

[50] Raymond Ong K J. An investigation of shaft current in a large sleeve bearing induction machine. Ph.D. Thesis. Hamilton (Canada): McMaster University, 1999.

[51] Hadden T, Jiang J W, Bilgin B, Yang Y Y, Sathyan A, Dadkhah H, Emadi A. A review of shaft voltages and bearing currents in EV and HEV motors. In *Proceedings of IECON 2016 - 42nd Annual Conference of the IEEE Industrial Electronics Society*, Florence, Italy, 2016: 1578–1583.

[52] Da Silveira Balestrin L B, Del Duque D, Da Silva D S, Galembeck F. Triboelectricity in insulating polymers: Evidence for a mechanochemical mechanism. *Faraday Discuss* **170**: 369–383 (2014)

[53] Krein P T. Electrostatic discharge issues in electric vehicles. *IEEE Trans Ind Appl* **32**(6): 1278–1284 (1996)

[54] Abu-Rub H, Bayhan S, Moinoddin S, Malinowski M, Guzinski J. Medium-voltage drives: Challenges and existing technology. *IEEE Power Electron Mag* **3**(2): 29–41 (2016)

[55] Kempski A. Capacitively coupled discharging currents in bearings of induction motor fed from PWM (pulsewidth modulation) inverters. *J Electrosta* **51**–**52**: 416–423 (2001)

[56] Zhu J L, Kim H, Chen H, Erickson R, Maksimović D. High efficiency SiC traction inverter for electric vehicle applications. In *Proceedings of 2018 IEEE Applied Power Electronics Conference and Exposition*, San Antonio, TX, USA, 2018: 1428–1433.

[57] Arora T G, Renge M M, Aware M V. Effects of switching frequency and motor speed on common mode voltage, common mode current and shaft voltage in PWM inverter-fed induction motors. In *Proceedings of 2017 12th IEEE Conference on Industrial Electronics and Applications*, Siem Reap, Cambodia, 2017: 583–588.

[58] Muetze A, Binder A. Calculation of motor capacitances for prediction of the voltage across the bearings in machines of inverter-based drive systems. *IEEE Trans Ind Appl* **43**(3): 665–672 (2007)

[59] Schuster M, Binder A. Comparison of different inverter-fed AC motor types regarding common-mode bearing currents. In *Proceedings of 2015 IEEE Energy Conversion Congress and Exposition*, Montreal, QC, Canada, 2015: 2762–2768.

[60] Chen S T, Lipo T A. Circulating type motor bearing current in inverter drives. *IEEE Ind Appl Mag* **4**(1): 32–38 (1998)

[61] Plazenet T, Boileau T, Caironi C, Nahid-Mobarakeh B. A comprehensive study on shaft voltages and bearing currents in rotating machines. *IEEE Trans Ind Appl* **54**(4): 3749–3759 (2018)

[62] Bhattacharya S, Resta L, Divan D M, Novotny D W. Experimental comparison of motor bearing currents with PWM hard-and soft-switched voltage-source inverters. *IEEE Trans Power Electron* **14**(3): 552–562 (1999)

[63] Kriese M, Wittek E, Gattermann S, Tischmacher H, Poll G, Ponick B. Prediction of motor bearing currents for converter operation. In *Proceedings of the XIX International Conference on Electrical Machines*, Rome, Italy, 2010: 1–6.

[64] Muetze A, Binder A. Techniques for measurement of parameters related to inverter-induced bearing currents. *IEEE Trans Ind Appl* **43**(5): 1274–1283 (2007)

[65] Muetze A, Binder A. Don't lose your bearings. *IEEE Ind Appl Mag* **12**(4): 22–31 (2006)

[66] Busse D, Erdman J, Kerkman R J, Schlegel D, Skibinski G. System electrical parameters and their effects on bearing currents. *IEEE Trans Ind Appl* **33**(2): 577–584 (1997)

[67] Cen H, Lugt P M. Film thickness in a grease lubricated ball bearing. *Tribol Int* 134: 26–35 (2019)

[68] Bader N, Furtmann A, Tischmacher H, Poll G. Capacitances and lubricant film thicknesses of grease and oil lubricated bearings. *STLE Annual Meeting & Exhibition*, Atlanta, Georgia, USA, 2017.

[69] Magdun O, Gemeinder Y, Binder A. Investigation of influence of bearing load and bearing temperature on EDM bear*ing currents. In Proceedings of 2010 IEEE Energy Conversion Congress and Exposition*, Atlanta, GA, USA, 2010: 2733–2738.

[70] Kempski A. Capacitively coupled discharging currents in bearings of induction motor fed from PWM (pulsewidth modulation) inverters. *J Electrostat* **51**–**52**: 416–423 (2001)

[71] Mäki-Ontto P. Modeling and reduction of shaft voltages in AC motors fed by frequency converters. Ph.D. Thesis. Helsinki (Finland): Helsinki University of Technology, 2006.

[72] Asefi M, Nazarzadeh J. Survey on high-frequency models of PWM electric drives for shaft voltage and bearing current analysis. *IET Electr Syst Transp* **7**(3): 179–189 (2017)

[73] Maki-Ontto P, Luomi J. Induction motor model for the analysis of capacitive and induced shaft voltages. In *Proceedings of 2005 IEEE International Conference on Electric Machines and Drives*, San Antonio, TX, USA, 2005: 1653–1660.

[74] Muetze A, Binder A. Calculation of circulating bearing currents in machines of inverter-based drive systems. *IEEE Trans Ind Electron* **54**(2): 932–938 (2007)

[75] Stone G, Lloyd B, Sasic M. Monitoring of shaft voltages and grounding currents in rotating machines. In *Proceedings of 2014 17th International Conference on Electrical Machines and Systems*, Hangzhou, 2014: 3361–3364.

[76] Magdun O, Binder A. High-frequency induction machine modeling for common mode current and bearing voltage calculation. *IEEE Trans Ind Appl* **50**(3): 1780–1790 (2014)

[77] Boucenna N, Hlioui S, Revol B, Costa F. A detailed analysis of the propagation paths of high-frequency common mode currents in AC motors. In *Proceedings of 2013 15th European Conference on Power Electronics and Applications*, Lille, France, 2013: 1–6.

[78] Magdun O, Binder A. The high-frequency induction machine parameters and their influence on the common mode stator ground current. In *Proceedings of 2012 International Conference on Electrical Machines*, Marseille, France, 2012: 505–511.

[79] Bonnett A H. Cause and analysis of bearing failures in electrical motors. In *Proceedings of 1992 Record of Conference Papers Industry Applications Society 39th Annual Petroleum and Chemical Industry Conference*, San Antonio, TX, USA, 1992: 87–95.

[80] Prudhom A, Antonino-Daviu J, Razik H, Climente-Alarcon V. Time-frequency vibration analysis for the detection of motor damages caused by bearing currents. *Mech Syst Signal Process* **84**: 747–762 (2017)

[81] Sunahara K, Ishida Y, Yamashita S, Yamamoto M, Nishikawa H, Matsuda K, Kaneta M. Preliminary measurements of electrical micropitting in grease-lubricated point contacts. *Tribol Trans* **54**(5): 730-735(2011).

[82] Yu Z Q, Yang Z G. Fatigue failure analysis of a grease-lubricated roller bearing from an electric motor. *J Fail Anal Prev* **11**(2): 158–166 (2011)

[83] Xie G X, Luo J B, Liu S H, Zhang C H, Lu X C. Micro-bubble phenomenon in nanoscale water-based lubricating film induced by external electric field. *Tribol Lett* **29**(3): 169–176 (2008)

[84] Nanayakkara Y S, Perera S, Bindiganavale S, Wanigasekara E, Moon H, Armstrong D W. The effect of AC frequency on the electrowetting behavior of ionic liquids. *Anal Chem* **82**(8): 3146–3154 (2010)

[85] Costello M J. Shaft voltages and rotating machinery. In *Proceedings of 1991 Industry Applications Society 38th Annual Petroleum and Chemical Industry Conference*, Toronto, Ontario, Canada, 1991: 71–78.

[86] Chatterton S, Pennacchi P, Vania A. Electrical pitting of tilting-pad thrust bearings: Modelling and experimental evidence. *Tribol Int* **103**: 475–486 (2016)

[87] Oliver J A, Guerrero G, Goldman J. Ceramic bearings for electric motors: eliminating damage with new materials. *IEEE Ind Appl Mag* **23**(6): 14–20 (2017）

[88] Suzumura J. Prevention of electrical pitting on rolling bearings by electrically conductive grease. *Quart Rep RTRI* **57**(1): 42–47 (2016)

[89] Komatsuzaki S, Uematsu T, Itoh R. A study of antielectrowear properties of lubricating greases from the viewpoint of grease composition. *J Japan Soc Lubr Eng* **28**(1): 54–60 (1983)

[90] Chiou Y C, Lee R T, Lin C M. Formation criterion and mechanism of electrical pitting on the lubricated surface under AC electric field. *Wear* **236**(1–2): 62–72 (1999)

[91] Liu W. The prevalent motor bearing premature failures due to the high frequency electric current passage. *Eng Fail Anal* **45**: 118–127 (2014)

[92] Prashad H. Determination of time span for the appearance of flutes on the track surface of rolling-element bearings under the influence of electric current. *Tribol Trans* **41**(1): 103–109 (1998)

[93] Ong R, Dymond J H, Findlay R D, Szabados B. Systematic practical approach to the study of bearing damage in a large oil-ring-lubricated induction machine. *IEEE Trans Ind Appl* **36**(6): 1715–1724 (2000)

[94] Didenko T, Pridemore W D. Electrical fluting failure of a Tri-lobe roller bearing. *J Fail Anal Prev* **12**(5): 575–580 (2012)

[95] Raadnui S, Kleesuwan S. Electrical pitting wear debris analysis of grease-lubricated rolling element bearings. *Wear* **271**(9–10): 1707–1718 (2011)

[96] Xie G X, Luo J B, Guo D, Liu S H, Li G. Damages on the lubricated surfaces in bearings under the influence of weak electrical currents. *Sci China Technol Sci* **56**(12): 2979–2987 (2013)

[97] Xie G X, Guo D, Luo J B. Lubrication under charged conditions. *Tribol Int* **84**: 22–35 (2015)

[98] Xie G X, Si L N, Guo D, Liu S H, Luo J B. Interface characteristics of thin liquid films in a charged lubricated contact. *Surf Interface Anal* **47**(3): 315–324 (2015)

[99] Zhang L, Xie G X, Wu S, Peng S G, Zhang X Q, Guo D, Wen S Z, Luo J B. Ultralow friction polymer composites incorporated with monodispersed oil microcapsules. *Friction*, in Press, doi 10.1007/s40544-019-0312-4.

[100] Wang W, Xie G X, Luo J B. Black phosphorus as a new lubricant. *Friction* **6**(1): 116–142 (2018)

[101] Wong V W, Tung S C. Overview of automotive engine friction and reduction trends–Effects of surface, material, and lubricant-additive technologies. *Friction* **4**(1): 1–28 (2016)

[102] Romanenko A, Muetze A, Ahola J. Effects of electrostatic discharges on bearing grease dielectric strength and composition. *IEEE Trans Ind Appl* **52**(6): 4835–4842 (2016)

[103] Huang P, Guo D, Xie G X, Li J. Electromechanical

failure of MoS_2 nanosheets. *Phys Chem Chem Phys* **20**(27): 18374–18379 (2018)

[104] Chen Z W, Guo D, Si L N, Xie G X. Nanotribological properties of graphite intercalation compounds: AFM studies. *Scanning* **2017**: 9438573 (2017)

[105] Komatsuzaki S, Uematsu T, Kobayashi Y. Change of grease characteristics to the end of lubricating life. *NLGI Spokesm* **63**: 22–27 (2000)

[106] Luo J B, He Y, Zhong M, Jin Z M. Gas bubble phenomenon in nanoscale liquid film under external electric field. *Appl Phys Lett* **89**(1): 013104 (2006)

[107] Xie G X, Luo J B, Liu S H, Zhang C H, Lu X C, Guo D. Effect of external electric field on liquid film confined within nanogap. *J Appl Phys* **103**(9): 094306 (2008)

[108] Xie G X, Luo J B, Liu S H, Guo D, Zhang C H. Bubble generation in a nanoconfined liquid film between dielectric-coated electrodes under alternating current electric fields. *Appl Phys Lett* **96**(22): 223104 (2010)

[109] Xie G X, Luo J B, Liu S H, Guo D, Li G, Zhang C H. Effect of liquid properties on the growth and motion characteristics of micro-bubbles induced by electric fields in confined liquid films. *J Phys D*: *Appl Phys* **42**(11): 115502 (2009)

[110] Mugele F, Baret J C. Electrowetting: From basics to applications. *J Phys*: *Condens Matter* **17**(28): R705–R774 (2005)

[111] McHale G, Orme B V, Wells G G, Ledesma-Aguilar R. Apparent contact angles on lubricant-impregnated surfaces/SLIPS: From superhydrophobicity to electrowetting. *Langmuir* **35**(11): 4197–4204 (2019)

[112] Xie G X, Luo J B, Liu S H, Guo D, Zhang C H, Si L N. Electrospreading of dielectric liquid menisci on the small scale. *Soft Matter* **7**(13): 6076–6081 (2011)

[113] Yang H M, Li J S, Zeng X Q. Tribological behavior of nanocarbon materials with different dimensions in aqueous systems. *Friction*, in Press, doi 10.1007/s40544-018-0235-5.

[114] Thiam A R, Bremond N, Bibette J. Breaking of an emulsion under an ac electric field. *Phys Rev Lett* **102**(18): 188304 (2009)

[115] Staicu A, Mugele F. Electrowetting-induced oil film entrapment and instability. *Phys Rev Lett* **97**(16): 167801 (2006)

[116] Lee T S, Chang J S. Electrohydrodynamic surface waves of thin oil films generated by needle–plate barrier discharges under reduced gas pressures. *J Electrostat* **51**–**52**: 565–570 (2001)

[117] Xie G X, Yang Y, Luo J B, Guo D, Si L N. AC pulse dielectric barrier corona discharge over oil surfaces: Effect of oil temperature. *IEEE Trans Plasma Sci* **41**(3): 481–484 (2013)

[118] Xie G X, Luo J B, Liu S H, Guo D, Zhang C H. "Freezing" of nanoconfined fluids under an electric field. *Langmuir* **26**(3): 1445–1448 (2010)

[119] Kolodziejczyk L, Martinez-Martinez D, Rojas T C, Fernández A, Sánchez-López JC. Surface-modified Pd nanoparticles as a superior additive for lubrication. *J Nanopar Res* **9**(4): 639–645 (2007)

[120] Fan X Q, Xia Y Q, Wang L P. Tribological properties of conductive *lubrica***t**ing greases. *Friction* **2**(4): 343–353 (2014)

[121] Park J Y, Salmeron M. Fundamental aspects of energy dissipation in friction. *Chem Rev* **114**(1): 677–711 (2014)

[122] Ma L R, Luo J B. Thin film lubrication in the past 20 years. *Friction* **4**(4): 280–302 (2016)

[123] Luo J B, Shen M W, Wen S Z. Tribological properties of nanoliquid film under an external electric field. *J Appl Phys* **96**(11): 6733–6738 (2004)

[124] Meng Y G, Hu B, Chang Q Y. Control of local friction of metal/ceramic contacts in aqueous solutions with an electrochemical method. *Wear* **260**(3): 305–309 (2006)

[125] Senouci A, Frene J, Zaidi H. Wear mechanism in graphite–copper electrical sliding contact. *Wear* **225**–**229**: 949–953 (1999)

[126] Drummond C. Electric-field-induced friction reduction and control. *Phys Rev Lett* **109**(15): 154302 (2012)

[127] Sweeney J, Hausen F, Hayes R, Webber G B, Endres F, Rutland M W, Bennewitz R, Atkin R. Control of nanoscale friction on gold in an ionic liquid by a potential-dependent ionic lubricant layer. *Phys Rev Lett* **109**(15): 155502 (2012)

[128] Chang Q Y. Investigation of the mechanism of voltage-controlled friction of metal/ceramic sliding couples in aqueous solutions. Ph.D. Thesis. Beijing (China): Tsinghua University, 2003.

[129] Park J Y, Qi Y B, Ogletree D F, Thiel P A, Salmeron M. Influence of carrier density on the friction properties of silicon *pn* junctions. *Phys Rev B* **76**(6): 064108 (2007)

[130] Wang J J, Li J M, Li C, Cai X L, Zhu W G, Jia Y. Tuning the nanofriction between two graphene layers by external electric fields: A density functional theory study. *Tribol Lett* **61**(1): 4 (2016)

[131] Apodaca M M, Wesson P J, Bishop K J M, Ratner M A, Grzybowski B A. Contact electrification between identical materials. *Angew Chem Int Ed* **49**(5): 946–949 (2010)

[132] Yamamoto Y, Kato O, Moue T, Kikuma T, Yamamoto T.

Characteristics of high temperature tribology of plasma sprayed WC-12Co coatings. *Pureitingu to Kotingu* **9**(6): 321–328 (1989)

[133] Chen R J, Zhai W J, Qi Y L. The Mechanism and technology of friction control by applying electric voltage II. The effects of applied *voltage on friction. Tribology* **16**(3): 235–238 (1996)

[134] Zhai W J, Chen R J, Qi Y Y. The mechanism and technique of friction control by applied voltage I. The correlation of self-generated voltage to friction force. *Tribology* **16**(1): 1–5 (1996)

[135] Goto K. The influence of surface induced voltage on the wear mode of stainless steel. *Wear* **185**(1–2): 75–81 (1995)

[136] Hurricks P L. The effect of applied voltage on the frictional behaviour of carbon black filled elastomers. *Wear* **52**(2): 365–380 (1979)

[137] Petrenko V F. The effect of static electric fields on ice friction. *J Appl Phys* **76**(2): 1216–1219 (1994)

[138] Arakawa M, Petrenko V F, Chen C. Effect of direct- and alternating-current electric fields on friction between ice and metals. *Can J Phys* **81**(1–2): 209–216 (2003)

[139] Seto T. Effects of an electric field on the static friction of a metal on a ferroelectric material. *Appl Phys Lett* **67**(3): 442–443 (1995)

[140] Ding T, Chen G X, Shen M X, Zhu M H, Zhang W H. Effect of arc discharge on friction and wear behaviors of stainless steel/copper-impregnated metalized carbon couple under electric current. *Adv Mater Res* **150–151**: 1364–1368 (2010)

[141] Zeng Y M, He F, Wang Q, Yan X H, Xie G X. Friction and wear behaviors of molybdenum disulfide nanosheets under normal electric field. *Appl Surf Sci* **455**: 527–532 (2018)

[142] Conache G, Ribayrol A, Fröberg L E, Borgström M T, Samuelson L, Montelius L, Pettersson H, Gray S M. Bias-controlled friction of InAs nanowires on a silicon nitride layer studied by atomic force microscopy. *Phys Rev B* **82**(3): 035403 (2010)

[143] Jiang Y, Yue L L, Yan B S, Liu X, Yang X F, Tai G A, Song J. Electric control of friction on silicon studied by atomic force microscope. *Nano* **10**(3): 1550038 (2015)

[144] Mukherjee A, Craciun A D, Gallani J L, Rastei M V. Nanoscale adhesion and sliding on biased semiconductors. *Faraday Discuss* **199**: 323–334 (2017)

[145] Liu H W, Fujisawa S, Tanaka A, Enomoto Y. Controlling and improving the microtribological properties of langmuir–blodgett monolayer films using an external electric field. *Thin Solid Films* **368**(1): 151–155 (2000)

[146] Csapo E, Zaidi H, Paulmier D. Friction behaviour of a graphite-graphite dynamic electric contact in the presence of argon. *Wear* **192**(1–2): 151–156 (1996)

[147] Lavielle L. Electric field effect on the friction of a polyethylene-terpolymer film on a steel substrate. *Wear* **176**(1): 89–93 (1994)

[148] Jiang Y, Li Y, Liang B, Yang X F, Han T W, Wang Z. Tribological behavior of a charged atomic force microscope tip on graphene oxide films. *Nanotechnology* **23**(49): 495703 (2012)

[149] Karuppiah K S K, Zhou Y B, Woo L K, Sundararajan S. Nanoscale friction switches: Friction modulation of monomolecular assemblies using external electric fields. *Langmuir* **25**(20): 12114–12119 (2009)

[150] Herminghaus S. A Generic Mechanism of sliding friction between charged soft surfaces. *Phys Rev Lett* **95**(26): 264301 (2005)

[151] Xie G X, Luo J B, Liu S H, Guo D, Zhang C H. Thin liquid film lubrication under external electrical fields: Roles of liquid intermolecular interactions. *J Appl Phys* **109**(11): 114302 (2011)

[152] Fajardo O Y, Bresme F, Kornyshev A A, Urbakh M. Electrotunable friction with ionic liquid lubricants: How important is the molecular structure of the ions. *J Phys Chem Lett* **6**(20): 3998–4004 (2015)

[153] Cooper P K, Li H, Rutland M W, Webber G B, Atkin R. Tribotronic control of friction in oil-based lubricants with ionic liquid additives. *Phys Chem Chem Phys* **18**(34): 23657–23662 (2016)

[154] Li H, Rutland M W, Watanabe M, Atkin R. Boundary layer friction of solvate ionic liquids as a function of potential. *Faraday Discuss* **199**: 311–322 (2017)

[155] Wada M, Yamada K, Kameyama T, Yamada N, Yoshida K, Saito A, Makino M, Khosla A, Kawakami M, Furukawa H. Electric control of friction on surface of high-strength hydrogels. *Microsyst Technol* **24**(1): 639–646 (2018)

[156] Jiang H J, Meng Y G, Wen S Z, Ji H. Effects of external electric fields on frictional behaviors of three kinds of ceramic/metal rubbing couples. *Tribol Int* **32**(3): 161–166 (1999)

[157] Zhai W J, Tian Y, Wang C. The voltage-controlled friction performance of GCr15/45 Steel rubbing pairs lubricated by 0.4% aluminum stearate fluid. *Lubr Eng* **5**: 23–25 (2004)

[158] Paulmier D, El Mansori M, Zaïdi H. Study of magnetized or electrical sliding contact of a steel XC48/graphite couple. *Wear* **203–204**: 148–154 (1997)

[159] Lin X Z, Zhu M H, Mo J L, Chen G X, Jin X S, Zhou Z R. Tribological and electric-arc behaviors of carbon/copper

pair during sliding friction process with electric current applied. *Trans Nonferr Met Soc China* **21**(2): 292–299 (2011)

[160] Csapo E, Zaidi H, Paulmier D, Kadiri E K, Bouchoucha A, Robert F. Influence of the electrical current on the graphite surface in an electrical sliding contact. *Surf Coat Technol* **76–77**: 421–424 (1995)

[161] Umehara N, Yamamoto T. Friction control between CNx coating and stainless steel ball with electric field. In *Proceedings of IEEE International Symposium on Micro-Nano Mechatronics and Human Science*, Nagoya, Japan, 2015: 213–216.

[162] Park, J Y, Ogletree D F, Thiel P A, Salmeron M. Electronic Control of Friction in Silicon pn Junctions. *Science* **313**(5784): 186 (2006)

[163] Schiferl R F, Melfi M J. Bearing current remediation options. *IEEE Ind Appl Mag* **10**(4): 40–50 (2004)

[164] Willwerth A, Roman M. Electrical bearing damage—A lurking problem in inverter-driven traction motors. In *Proceedings of 2013 IEEE Transportation Electrification Conference and Expo*, Detroit, MI, USA, 2013: 1–4.

[165] Chmelik K, Cech V, Foldyna J. Devices for prevention of bearings devaluation by electric current. In *Proceedings of 2007 IEEE International Symposium on Diagnostics for Electric Machines*, *Power Electronics and Drives*, Cracow, Poland, 2007: 316–319.

[166] Akagi H, Tamura S. A passive EMI filter for eliminating both bearing current and ground leakage current from an inverter-driven motor. *IEEE Trans Power Electron* **21**(5): 1459–1469 (2006)

[167] Hedayati M H, Acharya A B, John V. Common-mode filter design for PWM rectifier-based motor drives. *IEEE Trans Power Electron* **28**(11): 5364–5371 (2013)

[168] Pairodamonchai P, Suwankawin S, Sangwongwanich S. Design and implementation of a hybrid output EMI filter for high-frequency common-mode voltage compensation in PWM inverters. *IEEE Trans Ind Appl* **45**(5): 1647–1659 (2009)

[169] Ala G, Giaconia G C, Giglia G, Di Piazza M C, Vitale G. Design and performance evaluation of a high power-density EMI filter for PWM inverter-fed induction-motor drives. *IEEE Trans Ind Appl* **52**(3): 2397–2404 (2016)

[170] Voldoire A, Schanen J L, Ferrieux J P, Gautier C, Saber C. Optimal design of an AC filtering inductor for a 3-phase PWM inverter including saturation effect. In *Proceedings of 2019 10th International Power Electronics*, *Drive Systems and Technologies Conference*, Shiraz, Iran, 2019: 595–599.

[171] Han Y, Lu H F, Li Y D, Chai J Y. Analysis and suppression of shaft voltage in SiC-based inverter for electric vehicle applications. *IEEE Trans Power Electron* **34**(7): 6276–6285 (2019)

[172] Un E, Hava A M. A near-state PWM method with reduced switching losses and reduced common-mode voltage for three-phase voltage source inverters. *IEEE Trans Ind Appl* **45**(2): 782–793 (2009)

[173] Magdun O, Gemeinder Y, Binder A. Prevention of harmful EDM currents in inverter-fed AC machines by use of electrostatic shields in the stator winding overhang. In *Proceedings of IECON 2010 - 36th Annual Conference on IEEE Industrial Electronics Society*, Glendale, AZ, USA, 2010: 962–967.

[174] Busse D F, Erdman J M, Kerkman R J, Schlegel D W, Skibinski G L. An evaluation of the electrostatic shielded induction motor: A solution for rotor shaft voltage buildup and bearing current. *IEEE Trans Ind Appl* **33**(6): 1563–1570 (1997)

[175] Muetze A, Sullivan C R. Simplified design of common-mode chokes for reduction of motor ground currents in inverter drives. *IEEE Trans Ind Appl* **47**(6): 2570–2577 (2011)

[176] White M. Bearing ring with insulating coating. U.S. Patent 15 091 025, Oct. 2017.

[177] White M. Vapor deposition bearing coating. U.S. Patent 15 599 016. Nov. 2018.

[178] Muetze A, Binder A. Practical rules for assessment of inverter-induced bearing currents in inverter-fed AC motors up to 500 kW. *IEEE Trans Ind Electron* **54**(3): 1614–1622 (2007)

[179] Kuo M C, Hoover W R, Akkala M W, Mehlhorn W L. Conductive greases and methods for using conductive greases in motors. U.S. Patent 10 645 420. Mar. 2005.

[180] Oh W. White Paper: Preventing VFD/AC drive-induced electrical damage to AC motor bearings. https:// est-aegis.com/ TechPaper.pdf, 2018.

[181] Zhang P L, Wang G G, Zhao Y J, Wu H, Xia Y Q. Study of conductive and friction properties of grease containing carbon black additive. *Adv Mater Res* **1120–1121**: 586–589 (2015)

[182] Holm R. *Electric Contacts*: *Theory and Application*. 4th ed. Berlin (Germany): Springer, 2000.

[183] Li H Y, Wang X H, Guo X H, Yang X H, Liang S H. Material transfer behavior of $AgTiB_2$ and $AgSnO_2$ electrical contact materials under different currents. *Mater Des* **114**: 139–148 (2017)

[184] Fujishige M, Sekino M, Fujisawa K, Morimoto S, Takeuchi K, Arai S, Kawai A. Electric contact characteristic under low load of silver-carbon nanotube composite plating film corroded using H_2S gas. *Appl Phys Express* **3**(6): 065801 (2010)

[185] Li Y H, Zhang H Y, Wu B W, Guo Z. Improving the oxidation resistance and stability of Ag nanoparticles by coating with multilayered reduced graphene oxide. *Appl Surf Sci* **425**: 194–200 (2017)

[186] Sundberg J, Mao F, Andersson A M, Wiklund U, Jansson U. Solution-based synthesis of AgI coatings for low-friction applications. *J Mater Sci* **48**(5): 2236–2244 (2013)

[187] Akbulut H, Hatipoglu G, Algul H, Tokur M, Kartal M, Uysal M, Cetinkaya T. Co-deposition of Cu/WC/graphene hybrid nanocomposites produced by electrophoretic deposition. *Surf Coat Technol* **284**: 344–352 (2015)

Feng HE. He received his bachelor degree in mechanical engineering in 2016 from Tsinghua University, Beijing, China. He is currently a Ph.D. candidate at the State Key Laboratory of Tribology of Tsinghua University. His research interests include the lubrication under charged conditions, electrically-controlled friction, and nanoscale friction.

Guoxin XIE. He received his Ph.D. degree at Tsinghua University, China, in 2010, majoring in mechanical engineering. After that, he spent two years at State Key Laboratory of Tribology, Tsinghua University, China for postdoctoral research. From 2012 to 2014, he worked at Royal Institute of Technology, Sweden, for another two-year post-doctoral research. Since 2014, he has worked at Tsinghua University as an associate professor. His research interests include intelligent self-lubrication, electric contact lubrication, etc. He has published more than 50 referred papers in the international journals. He won several important academic awards, such as Chinese Thousands of Young Talents, the Excellent Doctoral Dissertation Award of China, and Ragnar Holm Plaque from KTH, Sweden.

Jianbin LUO. He received his BEng degree from Northeastern University in 1982, and got his MEng degree from Xi'an University of Architecture and Technology in 1988. In 1994, he received his Ph.D. degree from Tsinghua University and then joined the faculty of Tsinghua University. Prof. Jianbin Luo is an academician of the Chinese Academy of Sciences and a Yangtze River Scholar Distinguished Professor of Tsinghua University, Beijing, China. He was awarded the STLE International Award (2013), the Chinese National Technology Progress Prize (2008), the Chinese National Natural Science Prize (2001), and the Chinese National Invention Prize (1996). Prof. Luo has been engaged in the research of thin film lubrication and tribology in nanomanufacturing. He has been invited as a keynote or plenary speaker for 20 times on the international conferences.